www.aem-journal.com

# Tooling in Spark Plasma Sintering Technology: Design, Optimization, and Application

Alexander M. Laptev,\* Martin Bram, Dariusz Garbiec, Jan Räthel, Antoine van der Laan, Yannick Beynet, Jens Huber, Matthias Küster, Marco Cologna, and Olivier Guillon

Spark plasma sintering as the prominent field-assisted sintering technique (FAST/SPS) is a novel technology for the rapid, pressure-assisted consolidation of powder materials. The main feature of FAST/SPS is the direct Joule heating of the applied tooling. Tooling is a challenging part of the FAST/SPS setup, which must withstand high pressure at elevated temperatures and ensure a uniform temperature distribution in the sintered part. This review looks at the standard FAST/SPS tooling, the specific tooling for sintering complex-shaped parts, and for pressureless sintering. A particular focus lies on graphite, the commonly used tooling material, and on alternative materials such as steel, alloys, ceramics, and composites. The review also considers the add-on tooling elements, such as spacers, foils, and thermal insulation. Furthermore, the article discusses the basics of FAST/SPS modeling, and the computer-based optimization of FAST/SPS tooling, the procedure used, and the modeling accuracy. The review briefly describes the tooling and equipment for manufacturing upsized parts and large-scale production. In addition, the article considers the tooling for FAST/SPS sintering under high pressure (up to 1 GPa) and ultra-high pressure (over 1 GPa). The article concludes with an analysis of the challenges and prospectives for the smart design of FAST/SPS tooling.

1. Introduction

Pressing and sintering are key operations in ceramic and powder technologies. Pressing and sintering are usually two separate operations in the processing chain. However, some technologies combine these operations in one step. The most common examples are hot isostatic pressing (HIP) and hot pressing (HP). In both cases, an external pressure supports powder forming and sintering. Sintering by HIP and HP is time-intensive due to slow radiation heating from the external thermal elements. HP with inductive heating enables faster heating. However, the fixed inductor size limits the tool diameter and tooling design. An alternative way of warming up is direct heating by electric current passing through the tooling and the sintered part. Literature defines this type of heating as direct resistive or Joule heating. Researchers were already using Joule heating in the 19th century for the synthesis of ceramics in self-made HP devices. The commercialization of this process began in the second half of the 20th century with the development of special equipment in Japan, Germany, and USA. At that time, HP with direct Joule heating became known as spark plasma sintering (SPS). SPS belongs to the family of field-assisted

sintering techniques (FAST). That is why the more appropriate abbreviation FAST/SPS is nowadays in use. Many reviews describe the unique features of FAST/SPS technique.<sup>[1–4]</sup> However, none of them consider the FAST/SPS tooling in detail. At the same time, tooling is a central element and the most

A. M. Laptev, M. Bram, O. Guillon Institute of Energy and Climate Research – Materials Synthesis and Processing Forschungszentrum Jülich GmbH 52425 Jülich, Germany E-mail: a.laptev@fz-juelich.de

A. M. Laptev, D. Garbiec Materials Engineering Division Łukasiewicz Research Network – Poznań Institute of Technology 6 Ewarysta Estkowskiego St., Poznan 61-755, Poland

The ORCID identification number(s) for the author(s) of this article can be found under https://doi.org/10.1002/adem.202301391.

© 2023 The Authors. Advanced Engineering Materials published by Wiley-VCH GmbH. This is an open access article under the terms of the Creative Commons Attribution-NonCommercial License, which permits use, distribution and reproduction in any medium, provided the original work is properly cited and is not used for commercial purposes.

DOI: 10.1002/adem.202301391

J. Räthel
Sintering and Characterization Department
Fraunhofer Institute for Ceramic Technologies and Systemes
Winterbergstr. 28, Dresden 01277, Germany

A. van der Laan, Y. Beynet Norimat 51 Rue de l'Innovation, 31670 Labège, France

J. Huber, M. Küster Dr. Fritsch Sondermaschinen GmbH Dieselstr. 8, 70736 Fellbach, Germany

M. Cologna
European Commission
Joint Research Centre
Hermann-von-Helmholtz-Str. 1, 76344 Eggenstein-Leopoldshafen,
Germany

on Wiley Online Library for rules of use; OA articles are governed by the applicable Creative Commons

ADVANCED ENGINEERING MATERIALS

www.advancedsciencenews.com www.aem-journal.com

challenging part of the FAST/SPS setup. First, like with HP, a part of the FAST/SPS tooling has the same temperature as the sintered powder which can exceed 2000 °C. The FAST/ SPS tooling must be able to withstand the applied mechanical load at this temperature and not react with the sintered powder. The thermal expansion coefficient (TEC) of the FAST/SPS die material must be lower than that of the sintered material for the safe ejection of the sintered part. Moreover, the tool material must stand thermal shock during the fast cooling of sintered parts in the FAST/SPS furnace. Second, unlike HP, the FAST/SPS tooling must be electrically conductive. A significant difference between HP and FAST/SPS technology is the means of heating, that is, external heating by radiation from heating elements with HP and direct resistive heating with FAST/ SPS tooling. In contrasrt to HP, the radiation from the external tooling surfaces, leads to energy loss and the temperature inhomogenity inside the FAST/SPS setup. Thermal insulation and the optimization of the tooling design can address this challenge. Another difference between HP and FAST/SPS is the water cooling of load and current transmitting plungers (electrodes). Cooling is necessary due to the warming up of electrodes by passing current. The water cooling of the electrodes reduces the cooling duration in the FAST/SPS cycle and the entire time of the sintering process. However, the water cooling leads to a thermal gradient in both the tooling and the sintering part toward electrodes. Here, the additional thermal insulation and proper tooling design can reduce the thermal inhomogeneity. Finally, the industrialization of FAST/SPS technology requires a tooling with high productivity, enhanced wear resistance, a long lifetime, good machinability, and a low cost. This review summarizes the experience in addressing the aforementioned challenges for FAST/SPS tooling. The article concludes with an outlook for the smart design and proper application of FAST/SPS tooling, which is crucially important for the success of FAST/SPS technology.

# 2. Tooling Design

#### 2.1. Basic Configuration

Figure 1 shows a schematic of a typical FAST/SPS tooling. The tooling includes two electrically conductive punches and a electrically conductive or, in rare instances, nonconductive die. The application of a nonconductive die is possible only at the sintering of an electrically conductive powder. Two electrically conductive spacers adapt the size of the tooling to the space between the water-cooled electrodes. The regular material used for the punches, die, and spacers is an isostatically pressed graphite. However, the application of metals or ceramics is also possible. Graphite foils or the foils of other materials, placed between tool elements and the sintered powder, improve the thermal and electrical conductivity of contacts. Thermal insulation of the die (usually with graphite felt) and punches (with carbon fiberreinforced composite plates-CFRC) reduces heat loss and improves the homogeneity of the temperature inside the sintered part. An airtight chamber in the FAST/SPS device protects the tooling against oxidation by use of vacuum, argon, or nitrogen atmosphere. A pyrometer or a thermocouple measures the temperature at a reference point and sends the input signal to the proportional-integral-derivative (PID) controller for the tuning of the thermal cycle.

#### 2.2. Tooling for Simple-Shaped Parts

FAST/SPS combines pressing and sintering in one operation. Pressing entirely determines the final configuration of the sintered product. Sintering merely causes a certain dimensional shrinkage and densification. Conventional FAST/SPS machines have a single moving piston design . This configuration assumes the use of a single-action tooling or a tooling with the floating die and the production of single-level parts with a fixed cross-section.

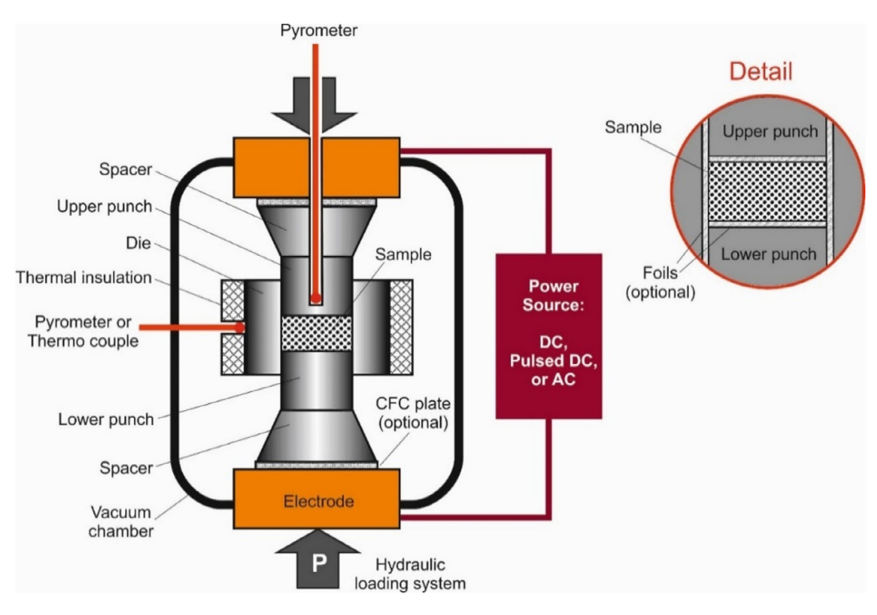
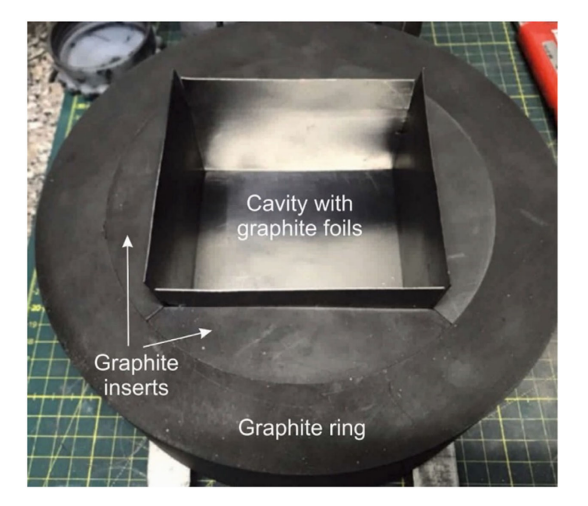


Figure 1. Schematic of a basic FAST/SPS setup and inserted foils. Courtesy of European Powder Metallurgy Association.

ons) on Wiley Online Library for rules of use; OA articles are governed by the applicable Creative Commons

www.aem-journal.com

Such parts belong either to class I or class II, according to the classification of the Metal Powder Industries Federation. The typical representatives of these classes are discs, rings, cylinders, plates, thin flat gears, and similar shapes.<sup>[5]</sup> However, sintering even these simple-shaped parts is challenging if their configuration differs from the thin disc. First, a large height or noncircular cross-section causes an additional temperature inhomogeneity inside the sintered part. Optimization of tooling design can solve this problem. To do so, the application engineers use their experience and intuition. However, the finite-element method (FEM)supported tooling design is more effective approach, especially for the newly developed parts. Second, sharp edges, such as in a rectangular part, lead to a stress concentration in the die wall and frequently to the die fracture. A solution for this problem is the application of a split die. Figure 2 shows an example of such a die with four graphite inserts in a graphite holding ring. The application of this die was the sintering of  $100 \times 100 \times 7 \text{ mm}^3$ tiles from a tungsten alloy used for the protection of the first wall in a fusion reactor. [6] Beside the reduction of die loading, the split die enables the easy extraction of the sintered tiles from the tool. However, its application requires additional time and costs for die manufacturing and the tooling assembling/disassembling before and after sintering, thus complicating the exploitation. Third, the FAST/SPS of parts with an internal hole (cylindrical or others) faces the problem of conflicting requirements for the TEC of tool materials. The die, punches, and core rod forming the internal hole, are typically from the identical material (e.g. graphite) to avoid thermal stresses or the appearance of gaps. At the same time, the TEC of the sintered material differs from that of the tooling material. To ensure the easy extraction of the sintered part, the TEC of the die material must be less than the TEC of the sintered material. However, the TEC of the core rod must be higher than that of the sintered part for the safe separation of the core rod and the sintered product. These requirements contradict each other if the materials of the core rod and the die are the same. Dr. Fritsch (Germany) developed the Tri-Force system, which can potentially solve this problem.<sup>[7,8]</sup> The Tri-Force design includes three hydraulic cylinders with independently moving pistons. This configuration enables



**Figure 2.** Split die for sintering square parts. Four inserts form the die cavity. Courtesy of Forschungszentrum Jülich GmbH.

the ejection of the sintered parts at elevated temperatures i.e. before cooling. However, only the limited information on the application of this system is available so far.

Despite the problems mentioned above, the literature provides examples of FAST/SPS sintering of parts with various single-level configurations, such as rectangular plates, hollow cylinders, and thin gears.  $^{[6,9,10]}$ 

#### 2.3. Tooling for Complex-Shaped Parts

The synthesis of complex-shaped parts in a standard FAST/SPS apparatus is a challenging task. The traditional powder metallurgy and ceramic industry applies the special adaptors or multipiston systems. [5] However, this approach is not feasible with the up-to-date FAST/SPS equipment with the single-piston design. The literature offers several papers describing the modification of FAST/SPS tooling to sinter parts with a complex geometry. The used approaches fall into five categories: 1) uniaxial loading in setup with several punches; 2) uniaxial loading using sacrificial insert; 3) field-assisted die forging; 4) quasi-isostatic pressing (QIP); and 5) pressure-free sintering.

#### 2.3.1. Uniaxial Loading

The fundamental problem with forming complex-shaped powder parts by uniaxial pressing is the internal friction in the powder media. The large internal friction restricts movement of powder particles in directions other than that of the applied pressure. Powder densification therefore mainly occurs in the direction of the acting load. Equation (1) evaluates the relative density along the corresponding line.

$$\rho = \rho_0 \times \frac{h_0}{h} \tag{1}$$

Here  $\rho_0$  and  $\rho$  are the relative densities before and after compaction;  $h_0$  and h are the heights of an arbitrary position of the cross-section before and after pressing. With  $h = h_0 - \Delta h$ , we get Equation (2).

$$\rho = \rho_0 \times \left(1 + \frac{\Delta h}{h}\right) \tag{2}$$

Here,  $\Delta h$  is the displacement of the punch. In a single-punch tooling,  $\Delta h$  is equal to the displacement of the electrode (Figure 1). The density of the compact varies across its cross-section following the change of the height h. If h is not constant, the density distribution is inhomogeneous. Subsequent sintering does not significantly change the uniformity of the density. Manière et al. credibly demonstrated the large density variation when sintering of a two-level alumina part in single-punch FAST/SPS tooling. [11]

Several Punches: A solution for homogeneous densification and sintering of multilevel parts in a regular FAST/SPS equipment is the use of tooling with several punches of different length. This design enables adjustment of punch displacement to the end height of the powder part. The density after sintering becomes homogeneous, if the relation  $\Delta h/h$  is the same across the entire cross-section (Equation (2)).

and-conditions) on Wiley Online Library for rules of use; OA articles are governed by the applicable Creative Commons

ENGINEERING

www.advancedsciencenews.com www.aem-journal.com

The literature offers a few papers describing the application of multipunch FAST/SPS tooling. Kubota et al. used double-punch tooling to sinter a zirconia can.<sup>[12]</sup> Voisin et al. achieved homogeneous densification using a set of punches with different length.<sup>[13]</sup> The authors demonstrated the sintering of a turbine blade made of IRIS (Ti<sub>48</sub>Al<sub>48</sub>W<sub>2</sub>Nb<sub>2</sub>) powder alloy.<sup>[14]</sup>

Sacrificial Insert: Manière et al. suggested an interesting solution for the uniform densification of a two-level part (**Figure 3**a). <sup>[15]</sup> The authors used a sacrificial insert to compensate the difference in height along the cross-section. Figure 3b shows the used setup schematically. The choice of alumina powder for both the sintered part and the sacrificial ring ensured their identical initial density and similar densification behavior. The key parameter in this setup is the height of the sacrificial ring. In accordance with Equation (1), the height ensuring the homogeneous densification of the entire sintered part is  $h_1 = h_2 - h_3$ . Here  $h_1$  is the height sacrificial ring,  $h_2$  is the total height of the part, and  $h_3$  is the height of the flange. Manière et al. verified this concept experimentally and found the homogeneous density and microstructure in the sintered part discussed. [15] The authors also admitted the main shortcomings of this approach: the limitation in the shape complexity of the sintered parts and the material losses due to the application of a sacrificial insert. The sacrificial insert was particularly adapted to produce ceramic gears by SPS.

Estournès et al. improved this method using a sacrificial insert with an imprint mimicking the shape of the sintered part. [16] The authors used the insert made of the same material as the material of the sintered part. The thin layer of BN deposited by spray or a graphite foil separated the insert and the powder part. This configuration ensures the well-predictable shrinkage and homogeneous densification of the sintered part in the regular FAST/SPS tooling. Manière et al. studied the application of this technique for manufacturing various complex-shaped parts including a CoNiCrAlY turbine blade. [17] Recently, Olevsky and Manière patented an advanced method for formation of separating interface between sacrificial and sintered powders. [18] The method assumes the use of a 3D-printed polymer shell filled with the sintered powder and embedded in the sacrificial powder medium. Thermal decomposition of polymer leads to appearance of a carbonous layer separating the sacrificial and sintered parts.

Field-Assisted Die Forging: Several papers describe the die forging of ceramics in a FAST/SPS apparatus. The researchers

used different mechanisms enabling the viscous flow in powder media. Shen et al. forged a conical part from an  $\alpha$ -sialon presintered sample in a graphite die at 1600 °C under a pressure of 20 MPa.<sup>[19]</sup> The α-sialon contained a small amount of viscous glassy phase, allowing the sliding of ceramic particles in a die cavity. Jiang et al. described the die forging of the Al<sub>2</sub>O<sub>3</sub>-ZrO<sub>2</sub>-MgAl<sub>2</sub>O<sub>4</sub> (AZM) composite at 1150 °C under a pressure of 105 MPa in a graphite tool. [20] The authors used a sintered disc as a starting preform. The final shape included small dimples with a height of around 1 mm. Jiang et al. attributed the deformability of AZM to the superplasticity in ceramics.<sup>[20,21]</sup> The challenges at die forging of ceramics are the low strength of graphite and difficult-to-predict material flow. [22] A feasible alternative is to separate sintering and forging into two subsequent steps. This technology is known in the literature as FAST-Forge. [23,24] The first step of the FAST-Forge process assumes the consolidation of the starting powder into a dense billet with a simplified shape. The second step is the die forging of the powder billet to a nearnet-shape part. Weston, Jackson, and Pope describe the application of FAST-Forge for Ti-6Al-4V and other titanium alloys. [23,24] The same research group used this technology for recycling of Ti-6Al-4V swarf.[25]

#### 2.3.2. Quasi-Isostatic Pressing

The indirect loading through a granular pressure-transmitting medium (PTM) is another option for sintering complex-shaped parts in a standard FAST/SPS tooling. The process is to some extent similar to HIP used in classical powder metallurgy. The difference is in the application of a granular medium instead of gas for pressure transmission (Figure 4a) and in the direct Ioule heating at FAST/SPS instead by radiation at HIP. In contrast to gas or liquid, solid particles do not transmit pressure uniformly throughout the medium. Therefore, this process becomes the name quasi-HIP. Quasi-HIP of complex-shaped green parts in a preheated PTM has been known since the 1970s. [26,27] However, only several short publications describe this technology named it as Ceracon process.[28,29] Hocquet et al. adapted Ceracon technology for FAST/SPS.<sup>[30]</sup> The authors used the laser machining of presintered Al<sub>2</sub>O<sub>3</sub> cylinders and WC-12%Co green compacts to manufacture complex-shaped preforms. They sintered these parts by FAST/SPS in the graphite or SiC pressuretransmitting powder bed. Beynet and Epherre (Norimat SAS)

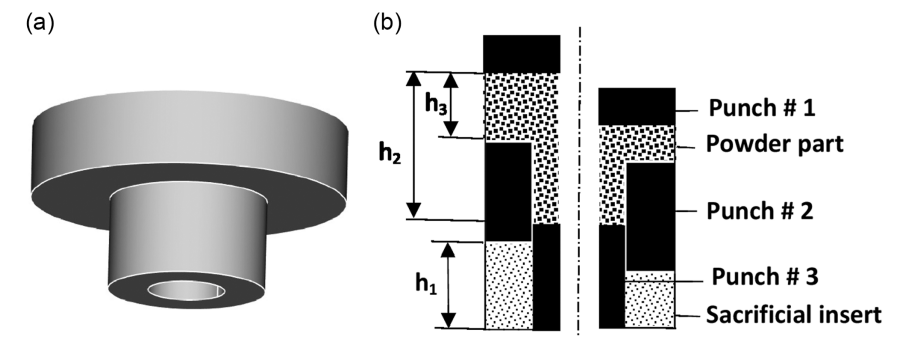


Figure 3. a) CAD drawing of two-level part and b) schematic view of FAST/SPS tooling with sacrificial ring: before sintering (left part) and after sintering (right part).

15272648, 2024, 5, Downloaded from https://onlinelibrary.wiley.com/doi/10.1002/adem.202301391 by Forschungszentrum Jülich GmbH Research Center, Wiley Online Library on [02:0572024]. See the Terms

ns) on Wiley Online Library for rules of use; OA articles are governed by the applicable Creative Commons

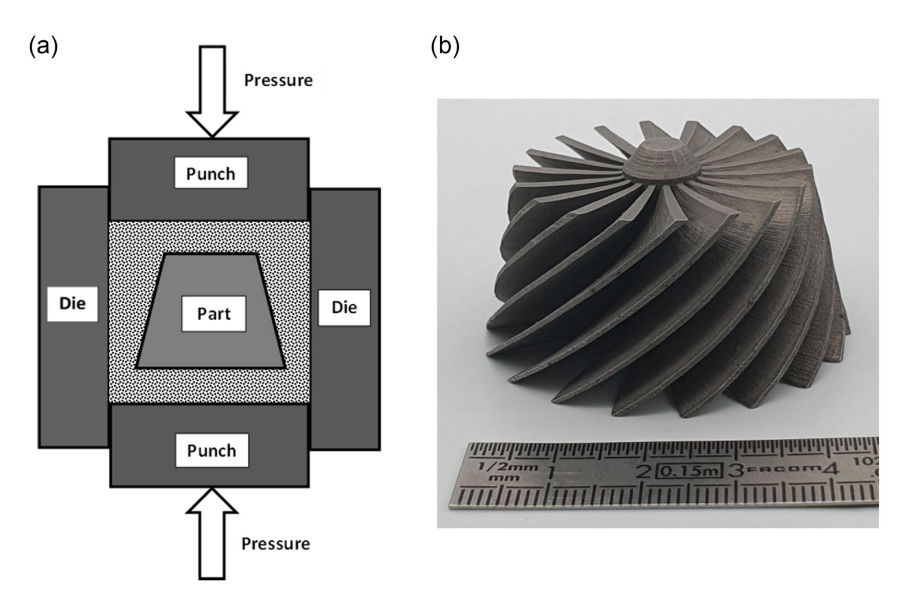
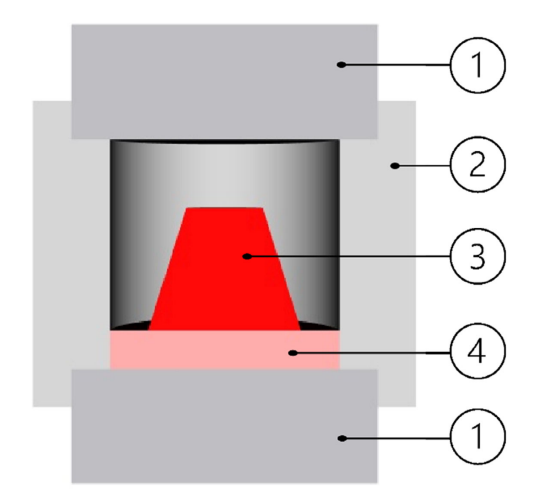


Figure 4. a) Schematic view of quasi-HIP in a PTM (dotted area); b) prototype of a turbine wheel shaped by 3D additive printing and sintered by quasi-HIP in FAST/SPS device. Courtesy of Norimat SAS.

patented the combination of 3D additive printing for shaping with subsequent sintering in PTM.<sup>[31]</sup> Figure 4b shows a prototype of a turbine wheel fabricated using this technology. The reported final porosity of the SS 316L part was less than 1%. The problems of quasi-HIP are the nonuniform shrinkage and the partial sintering of the pressure-transmitting powder.<sup>[30,32,33]</sup> The use of preforms with low shrinkage (e.g., preliminary sintered parts) addresses the problem of shape distortion. This approach makes quasi-HIP a suitable alternative to post-HIPing of additively manufactured shapes. Another option is FAST/SPS heat treatment without pressurization. This technique is known as pressure-less or pressure-free FAST/SPS sintering.

## 2.3.3. Pressure-Free FAST/SPS

A standard FAST/SPS tooling is easily transformable to tooling for pressure-free sintering by inserting a spacer between the upper and lower punches. Figure 5 shows the corresponding tooling design. Other tooling configurations are also possible.<sup>[34]</sup> This tooling is a kind of mini furnace with resistive heating. The application of pressure-free FAST/SPS is reasonable when a small load or contact with the tooling elements leads to the distortion of the part geometry or properties deterioration. For instance, Meng et al. used pressure-free FAST/SPS for the sintering of alumina microchannel parts produced by micropowder injection molding. [35] The pressure-free sintering preserved the geometry of channels. Dudina et al. applied this technology for the fabrication of porous iron aluminide by reactive sintering. In this paper, pressure-free sintering enabled open porosity. [36] Mishra et al. used pressure-free FAST/SPS in a graphite tooling to minimize the chemical and electrochemical reduction of gadolinium-doped ceria (GDC) due to interaction with the graphite electrodes. [37] However, a partial reduction of GDC apparently by residual carbon monoxide in the graphite tooling was still present. Dudina and Bokhonov observed similar results for



**Figure 5.** Schematic view of FAST/SPS tooling for pressure-free sintering: 1—punches (electrodes), 2—spacer (heating element), 3—sintered part, 4—support.

the pressure-free processing of a partially oxidized nickel powder.<sup>[38]</sup> The application of tooling materials alternative to graphite such as metals and alloys, ceramics, and composites can address this and other challenges of the FAST/SPS technology.

# 3. Tooling Materials

Tooling is the most challenging element of FAST/SPS units. As a rule, the temperature of the FAST/SPS die and punches is close to that of the sintered part. Therefore, the die, punch, and other tooling materials must meet several specific conditions. 1) Die and punch materials must withstand the applied pressure at a specified sintering temperature sometimes exceeding 2200 °C;

www.advancedsciencenews.com www.aem-journal.com

2) All tooling materials must not react with or contaminate the sintered material in direct or indirect contact with them; 3) The punches, and, in most cases, the die, must be electrically conductive up to the sintering temperature. The electrical resistivity of tooling must be constant or grow with temperature increase to avoid thermal-electrical runaway. The electrical conductivity of tooling materials should be in the range of that for graphite to generate sufficient Joule heat at low voltage and medium current; 4) The tooling materials (excluding thermal insulation) must have a moderate thermal conductivity ensuring fast heating and cooling with low thermal gradients and with acceptable heat loss; 5) The tooling materials must be resistant to thermal shock; 6) The tooling materials should have a low thermal expansion coefficient enabling easy ejection of sintered parts from the die; 7) The tooling materials must secure the acceptable change of clearance between tooling parts during exploitation; and 8) The tooling materials must be available on the market at an acceptable price.

None of the materials has fully met all these requirements. The application of graphite offers the best compromise.

#### 3.1. Graphite

Polycrystalline graphite is an electrical conductor with a moderate electrical resistivity in the range of 7.5–30  $\mu\Omega$  m. <sup>[39]</sup> Thus, the graphite parts can serve as heating elements. However, graphite reacts with oxygen at elevated temperatures. The application of graphite requires therefore an inert atmosphere or a vacuum environment. Graphite has moderate strength. However, in contrast to most materials, the strength of graphite grows with temperature up to 2500–2700 °C. A further rise in temperature leads to an abrupt decline in its strength. [40] Beside, graphite is prone to creep at elevated temperatures. [41,42] This is a crucial point when setting the FAST/SPS pressure, especially at hightemperature sintering. The manufacturers offer many grades of graphite varying in strength, electrical resistivity, thermal conductivity, and other properties. The research application shows the trend to use a fine-grained, isostatically pressed graphite with a compressive strength of 170-230 MPa. Table 1 summarizes some characteristics of these grades reported by manufacturers. [43-46] However, high-strength grades of graphite are extremely expensive. Industry prefers therefore cheaper grades with a lower strength. Accordingly, the usually recommended FAST/SPS pressure is between 30 and 50 MPa. Graphite has moderate thermal conductivity and thermal

**Table 1.** Properties of high-strength graphite at room temperature. [43–46]

Manufacturer, grade	SGL R7710	POCO ZXF-5Q	Mersen 2334	Schunk FE 879
Density [g cm <sup>-3</sup> ]	1.88	1.78	1.84	1.84
Electrical resistivity [ $\mu\Omega$ m]	13	19.5	20	25
Thermal conductivity [W $\mathrm{m}^{-1}$ $\mathrm{K}^{-1}$ ]	105	70	70	50
Modul of elasticity [GPa]	13.5	14.5	16	N/A
Flexural strength [MPa]	85	112	55	80
Compressive strength [MPa]	170	175	230	200
TEC·10 <sup>-6</sup> [K <sup>-1</sup> ]	4.7	8.1	6.0	5.2

diffusivity. Therefore, graphite heats up rapidly and cools down relatively fast with low thermal gradients. Heating of the graphite tooling is not energy consuming due to the low volumetric heat capacity of graphite. At the same time, graphite is an active reductant and carbide former reacting with many materials (W, Mo, Ti, oxides) at elevated temperatures. [47–49] The reactivity of graphite is a crucia point when setting the FAST/SPS thermal cycle. Graphite has a low friction coefficient but also a low wear resistance. Machining of graphite is easy but produces the fine dust. Graphite dust is hazardous and prone to fire and explosion. The employed lathe or milling machine must therefore have a dust collection system. The application of metallic and ceramic FAST/SPS tooling addresses some problems associated with graphite.

## 3.2. Steels and Alloys

Hot work tool steel is an option for manufacturing nongraphite FAST/SPS tooling. Within this class of steels, the preferred grades are those developed for long contact with hot surfaces e.g. during extrusion or die casting. Examples are QRO-90 Supreme (Uddeholm, Sweden), W-302 Isobloc (DIN 1.2344, AISI H13). and W-360 Isobloc (Böhler, Austria) steels. Table 2 presents the chemical composition of these steels reported by suppliers. [50–52] Table 3 compares the physical properties of W-360 steel with those of R7710 graphite at room temperature. In contrast to brittle graphite, steel is a ductile material with high strength at room temperature. However, the strength of the steels sharply decreases with temperature increase. Besides, the steels are prone to creep at elevated temperatures. The application area of steels is therefore below a temperature of around 550-600 °C. However, the steels allow a pressure of several hundred MPa at these temperatures. The drawback of steels is their low electrical resistivity, which can lead to an enhanced energy loss in the electrical circuit. Another drawback of tool steels is their low thermal conductivity and thermal diffusivity compared to graphite.

**Table 2.** Chemical composition of hot work tool steels used in FAST/SPS tooling. $^{[50-52]}$ 

Steel	С	Si	Mn	Cr	Мо	٧
QRO 90 Supreme	0.38	0.30	0.75	2.6	2.25	0.90
W-302 Isobloc	0.39	0.90	0.40	5.2	1.40	0.95
W-360 Isobloc	0.50	0.20	0.25	4.5	3.00	0.60

**Table 3.** Physical properties (RT) of steel, Ni, and Mo alloys versus properties of R7710 graphite.  $^{[43,52,53,142]}$ 

Material	W-360	Inco 718	TZM	R7710
Density [g cm <sup>-3</sup> ]	7.81	8.26	10.22	1.88
Electrical resistivity [ $\mu\Omega$ m]	0.59	1.18	0.05	13
Specific heat capacity [J $g^{-1} K^{-1}$ ]	0.43	0.46	0.25	0.72
Thermal conductivity [W m <sup>-1</sup> K <sup>-1</sup> ]	30.8	11.5	122	105
Thermal diffusivity [mm <sup>2</sup> s <sup>-1</sup> ]	9.17	3.03	47.7	77.6
Modulus of elasticity [GPa]	212	204	335	13.5
$TEC \cdot 10^{-6} [K^{-1}]$	10.8	14.1	5.2	4.7

www.advancedsciencenews.com www.aem-journal.com

This leads to the prolonged heating and cooling of the steel tooling. Heating of a steel tooling requires more energy compared to a graphite tooling with the same geometry. The reason for that is the higher volumetric heat capacity of tool steels compared to that of graphite. The steel elements conducting electrical current (e.g., punches and die) require a separating layer between them to prevent their welding. The literature describes some examples of steel tooling application for low-temperature sintering of Al alloys and ZnO. Section 7.1 considers this topic in more detail.

Ni-based superalloy is another option for FAST/SPS tooling. The inexpensive Inconel alloy 718 allows the use at temperatures of up to 700–750 °C. The more expensive Inconel 100 alloy or Astroloy alloy are applicable at temperatures of up to 900–950 °C. The drawbacks of nickel-based alloys are the same as that of hot work tool steels. Their electrical resistivity is higher than that of steel, but several times lower than the resistivity of graphite (Table 3). The thermal conductivity and thermal diffusivity of Ni-based superalloys are nearly three times lower than those of W-360 steel. The heating and cooling of the superalloy-based FAST/SPS tooling thus requires more time than the steel-based tooling. The Ni-based superalloys are also more difficult for machining compared with the steels. At present, the literature offers only limited information about the application of nickel superalloys in FAST/SPS tooling (see Section 7.1).

The molybdenum-based alloy TZM (0.5% Ti, 0.08% Zr, 0.03% C) is applicable at temperatures of up to 1100–1150 °C. TZM has a larger strength than the pure molybdenum and exhibits a higher recrystallization temperature (about 1400 °C) with better creep resistance. [53] The shortcoming of TZM is the low electrical resistivity. The thermal conductivity and thermal diffusivity of TZM are comparable with those of graphite (Table 3). However, TZM is  $\approx$ 10 times more expensive than Inconel 718. Section 7.1 considers several examples of TZM application in FAST/SPS tooling.

## 3.3. Ceramics and Composites

# 3.3.1. Ceramics

The literature describes examples of using conductive and nonconductive ceramics in FAST/SPS tooling (see Section 7.1). Table 4 presents the physical properties of these ceramics at room temperature. The binderless tungsten carbide (WC) possesses the electrical resistivity which is lower than that of W-360 steel and Inconel 718, but higher than the TZM alloy. However, the electrical resistivity of WC is around 60 times lower than the resistivity of R7710 graphite, and this is not optimal for heat generation. The thermal conductivity and thermal diffusivity of WC is higher than that of W-360 tool steel and Inconel 718, but lower than the conductivity and diffusivity of TZM and R7710 graphite. The upper-temperature limit for WC application has not been clear so far, but according to Aalund, it is around 1680 °C (0.6 of melting point in °C). [54] Silvestroni et al., reported for binderless WC a flexural strength of 1 GPa at 1500 °C. [55] Another ceramic material used in FAST/SPS tooling is silicon carbide (SiC). Silicon carbide is a semiconductor with electrical resistivity varying from that of graphite up to resistivity typical for insulating ceramics (Table 4). The electrical conductivity of SiC depends on the doping with boron, aluminum, or nitrogen, but in most cases, SiC tends to be an insulator. SiC is applicable as a die material in a regular FAST/SPS setup if the sintered material is electrically conductive. However, a special tooling design (discussed in Section 7.1) enables the use of punches manufactured from SiC ceramic as well. The thermal conductivity, thermal diffusivity, volumetric specific heat capacity, and flexural strength of  $\alpha$ -SiC are slightly below that of binderless WC. SiC maintains the high flexural strength up to  $\approx 1500 \, ^{\circ} \text{C}.^{[56]}$ Munro reported a flexural strength of 446 MPa for  $\alpha\textsc{-SiC}$  at this temperature. [57] However, the strength of SiC significantly depends on the production route used by the manufacturer. Leipold recommends the application of SiC punches in HP tool up to 1400 °C. [58] Boron carbide (B<sub>4</sub>C) is another prospective material for FAST/SPS tooling. At room temperature, B<sub>4</sub>C has thermal and mechanical properties identical to that of silicon carbide. At the same time, the electrical resistivity of B<sub>4</sub>C is much larger than the electrical resistivity of graphite (Table 4). B<sub>4</sub>C maintains a flexural strength of 400-600 MPa up to 1600 °C. [59]

The common shortcomings of ceramic tools are their brittleness, high cost, and pure machinability. The brittleness of ceramics restricts their application for the punches loaded by compressive pressure. The tensile stresses in a die can lead to its catastrophic failure due to the low tensile strength of ceramics. The brittleness of ceramics results in enhanced requirements regarding the parallelism of the punch ends and

Table 4. Physical properties of some ceramics and composites at room temperature.

Material	WC <sup>[143,144]</sup>	WC-6Co <sup>[61,145,146]</sup>	α-SiC <sup>[57]</sup>	B <sub>4</sub> C <sup>[143]</sup>	CFRC <sup>a)[67]</sup>
Density [g cm <sup>-3</sup> ]	15.8	14.9	3.16	2.52	1.6
Electrical resistivity [ $\mu\Omega$ m]	0.22	0.2	15-10 <sup>7[143]</sup>	10 <sup>3</sup> -10 <sup>5</sup>	123 <sup>[69]</sup>
Specific heat [J $g^{-1} K^{-1}$ ]	0.20	0.213	0.715	1.011	0.593 <sup>[70]</sup>
Therm. cond. [W $m^{-1} K^{-1}$ ]	63	80	114	30	5 <sup>[70]</sup>
Therm. diffusivity [mm² s <sup>-1</sup> ]	19.6	25.2	18.5	11.8	N/A
Flexural strength [MPa]	550	2000	359	310 <sup>[147]</sup>	230 <sup>b)</sup>
Fracture toughness [MPa m <sup>1/2</sup> ]	5.8	9.6	3.1	3.27 <sup>[147]</sup>	N/A
Modulus of elasticity [GPa]	620–720	590	415	450 <sup>[147]</sup>	75 <sup>b)</sup>
$TEC \cdot 10^{-6} [K^{-1}]$	5.2	5.0	5.12	4.3	7.3

<sup>&</sup>lt;sup>a)</sup>Perpendicular to alignment of fibers; <sup>b)</sup>Parallel to alignment of fibers. The grade Premium, SGL Carbon, Germany.

ADVANCED ENGINEERING

www.advancedsciencenews.com www.aem-journal.com

the entire loading system.<sup>[54]</sup> In addition, high heating and cooling rates, that are typical for FAST/SPS, can cause significant thermal stresses and failure of the ceramics due to their limited resistance to thermal shock. Although ceramics are low-reactive materials, their chemical interaction with sintered materials is possible. For instance, WC intensively reacts with Ti forming (W,Ti)C carbides.<sup>[60]</sup>

## 3.3.2. Composites

There are three reasons to use composites in FAST/SPS tooling: 1) to reduce ceramic brittleness; 2) to increase the electrical conductivity of the ceramics; and 3) to enhance fracture strength (for graphite-based composites). The application of cemented carbides, particularly WC-Co, addresses the first challenge (Section 7.1). The addition of cobalt to WC drastically increases the flexural strength and significantly enhances the fracture toughness of the WC-Co composite (Table 4). At the same time, the relatively low melting point of Co (1495 °C) restricts the application of the WC–Co composite to 1000–1050 °C. [61] The addition of a conductive filler to a nonconductive ceramic can address the second challenge (lack of electrical conductivity). The literature offers many options for fillers such as electrically conductive ceramics, carbon fibers, or carbon nanotubes. [62-65] However. little information is available regarding the application of such composites in FAST/SPS tooling. Räthel et al., added a graphite filler to WC and B<sub>4</sub>C ceramics, aiming to tailor their electrical conductivity. The authors achieved a resistivity of  $0.94\text{--}1.3\,\mu\Omega\,\text{m}$  for a WC-C composite and  $8.0\,\mu\Omega\,\text{m}$  for a B<sub>4</sub>C-C composite. [66] Unfortunately, the paper reported neither the chemical composition of FAST/SPS-synthesized materials nor their mechanical properties. Application of a special grade of graphite (as discussed in Section 3.1) or use of a graphitebased composite can address the third challenge (enhancement of graphite strength). One option is the application of CFRC, also known as carbon/carbon or C/C composite. The reinforcing phase in the pyrolytic graphite matrix is the wound carbon filaments (for CFRC cylinders) or a carbon cloth (for CFRC plates). CFRC composites are highly resistant to thermal gradients and thermal cycling. In a protective atmosphere, CFRCs retain their strength up to and above 2000 °C. [67] CFRCs are highly anisotropic in terms of thermal, electrical, and mechanical properties. The properties of CFRCs may vary over a wide range depending on the volumetric fraction of the reinforcer, the properties of the fiber and matrix, and the bonding between them. [68] Table 5 presents the physical properties of CFRC produced at SGL Carbon (Germany). [67,69,70] The electrical resistivity of this CFRC perpendicular to the alignment of the fibers is  $\approx$ 10 times

higher than that of R7710 graphite. However, this resistivity is low enough to enable the passing of a high-intensity current at a low voltage typical for FAST/SPS. The thermal conductivity of CFRC in this direction is significantly lower than that of R7710 graphite. Therefore, FAST/SPS tooling uses CFRC plates for thermal insulation (Section 4.3). The tensile strength of CFRC in the direction parallel to the alignment of the fibers is about 400 MPa. [67] The use of a CFRC cylinder for die thus appears to be reasonable. The compressive strength of CFRCs perpendicular to the alignment of the fibers is crucial to their application as punches. The manufacturers do not provide the values. However, Zheng et al., reported the application of a CFRC mold for the sintering of TaC at 2000 °C with a pressure of 200 MPa. [71] The shortcomings of CFRC are the high price and the low wear resistance.

# 4. Foils and Coatings, Insulation, Spacers

During FAST/SPS, not only the sintered material but also die and punches are at an elevated temperature. Therefore, the mechanical and chemical interaction between the sintered material and the tooling elements is a matter of consideration. Moreover, an elevated temperature of tool elements leads to heat loss due to radiation from the external surfaces and also to heat transfer toward the water-cooled electrodes. The application of separating foils, coatings, and thermal insulation addresses these problems.

## 4.1. Foils

The insertion of foils between the sintered material and the tool elements (Figure 1) improves the electrical and thermal contact of interfaces, creates the diffusion barrier, and protects the tooling surfaces from adhesion to the sintered material and mechanical damage. The foils must be soft, sufficiently thick, chemically inert, and easy to remove after sintering. Graphite foils meet most of these requirements. They are well-compressible, available in varying thicknesses, do not interact with graphite tooling, and are easy to remove by grinding, annealing in air, or sand-blasting. Table 5 presents some properties of a typical graphite foil. [43,70,72,73]

The graphite foil is a strongly anisotropic material. The foil thermal conductivity in plane (=) is slightly higher than that of R7710 graphite, and through the plane ( $^{\perp}$ ) it is as low as the thermal conductivity of zirconia. The electrical resistivity of graphite foil in plane is comparable to that of R7710 graphite, and through the plane it is much higher than the resistivity of

Table 5. Material data of graphite and graphite-based materials (all from SGL carbon) at room temperature.

Material	Grade	Thickness [mm]	m] Electrical resistivity [ $\Omega$ mm]		Thermal conductivity [W m <sup>-1</sup> K] <sup>-1</sup>	
	<u></u>	-	Т	=		=
Graphite <sup>[43]</sup>	R7710	-		13	1	05
Graphite foil <sup>[72]</sup>	TH	0.15–1	700	11	5	220
Graphite felt <sup>[73]</sup>	GFA10	9–10	3–4	1.5–2.5	0	05
CFRC <sup>[70]</sup>	1501 G	1.2–15	123	24	5	25

**ADVANCED** SCIENCE NEWS ADVANCED ENGINEERING MATERIALS

www.advancedsciencenews.com www.aem-journal.com

R7710 graphite. Graphite foil is inexpensive and easy in use. In some cases, graphite foil reacts with sintered material. A practical alternative might be the mica foil. Depending on the type, mica foil is usable in a temperature range from 650 to 1200 °C. Mica is an electrical insulator with the low thermal conductivity (below 0.5 W m $^{-1}$ °C $^{-1}$ ). The application of mica foil is therefore mainly suitable for sintering nonconductive materials. For example, Ihrig et al. used mica foil for the sintering of an electrochemical half-cell containing a LiCoO $_2$  layer which is prone to reduction by graphite. The use of refractory foils (W, Mo, Nb, or Ta) is effective for sintering at elevated temperatures. However, these foils are expensive, not easy in handle, and tend to interact or weld with many sintered materials.

#### 4.2. Coatings

An alternative approach to the separation of interfaces in FAS/ SPS tooling is the coating by spraying or brushing. The most common coatings in FAST/SPS practice are suspensions of hexagonal boron nitride (h-BN) or colloidal graphite. h-BN is a wellknown lubricant and a barrier-building agent used in many industries. h-BN is an electrical insulator, which can change the current path.<sup>[79]</sup> The tooling exploitation must consider this issue. In particular, the h-BN coating of a graphite mold creates a nonconductive layer. The maximum temperature for the application of h-BN (limited by decomposition) in a vacuum and reducing atmosphere is around 1400 °C. The research practice widely uses aerosol coating of graphite foil by h-BN spraying. In certain cases, colloidal graphite spraying can replace the graphite foil. The colloidal graphite does not significantly alter the electrical conductivity of the FAST/SPS tool. At the same time, it does not prevent a possible reaction with graphite or the carbon diffusion into the sintered material. A solution might be the use of graphite foil coated with a nonreactive conductive material.[80] However, even in such a case, the reducing environment inside the FAST/SPS die cannot fully exclude the interaction of the sintered material with carbon monoxide or CO2. [2]

#### 4.3. Thermal Insulation

In general, the FAST/SPS tooling is a kind of furnace with direct resistive heating. It is well-known that the effective exploitation of any furnace requires a proper thermal insulation. FAST/SPS utilizes two kinds of thermal insulation (Figure 1). The first is the graphite felt wrapped around the external die surface. The second is the CFRC inserts between the FAST/SPS tooling and the water-cooled electrodes.

#### 4.3.1. Graphite Felt

The insulation of the FAST/SPS tooling with graphite felt drastically reduces radiation from the heat-emitting surfaces. The low thermal conductivity of graphite felt (Table 5) results in the significant reduction of temperature of the external tooling surfaces. The effectiveness of thermal insulation grows with increasing sintering temperature according to the Stefan–Boltzmann law.

$$\dot{q}_{\rm r} = \varepsilon \times \sigma \times T_{\rm s}^4 \tag{3}$$

Here,  $\dot{q_r}$  is the heat flux due to radiation,  $\varepsilon$  is the emissivity,  $\sigma$  is the Stefan–Boltzmann constant, and  $T_S$  is the temperature of the radiating surface. It is worth noting that the large emissivity of graphite (around 0.8–0.9) results in the enhanced heat release. The experiments by Laptev et al., reveal a decrease in heating power of around 50% during sintering at 1375 °C after insulation of FAST/SPS tooling with graphite felt. [81] The thermal insulation is especially important when sintering in large molds and when the required sintering power approaches the limit of the power source. In addition, the thermal insulation significantly improves temperature homogeneity in the sintered part. [81]

## 4.3.2. CFRC

Typical CFRC insulation is a plate with low thermal conductivity (Table 5). The insertion of such a plate between the FAST/SPS tooling and the water-cooled electrode reduces the heat flux toward the electrodes. This measure may reduce the energy loss, which can be crucial when sintering in a large mold. In addition, the application of a CFRC insulation significantly reduces the thermal gradient along the vertical axis of the tooling. [69] This is important when sintering parts with a large height or sintering in multiple tools with vertically stacked layers. However, CFRC has a high electrical resistivity and therefore generates unused heat. The application of a CFRC insulation thus requires careful consideration. The FEM modeling of temperature inside the FAST/SPS setup is a good approach for the final decision.

#### 4.4. Spacers

Spacers are the elements of the FAST/SPS tooling separating the punches and the water-cooled electrodes (Figure 1). Spacers are usually conical but can be also cylindrical or rectangular. The spacer material is typically graphite, and sometimes metal (e.g., steel, TZM), or CFRC.<sup>[81–83]</sup> The geometry and material of the spacers significantly influence the temperature gradient toward the water-cooled electrodes. The proper spacer design often requires the FEM-based analysis .

# 5. Modeling and Optimization

An optimized tooling design is essential to the successful application of FAST/SPS technology. An unsuitable tooling design leads to an inhomogeneous sintering, enhanced energy consumption, overheating of the electrodes and the transformer, a long cooling time, the fracture of the tooling, and other technical and economic problems. The design of the FAST/SPS tooling is frequently based on previous experience, engineering intuition, or on the recommendations of manufacturers of FAST/SPS equipment. This approach works well for sintering small samples in a laboratory or at regular production. However, it becomes inefficient when upsizing or upscaling FAST/SPS production. The substantial number of factors influencing the FAST/SPS process makes the proper tooling design difficult without preliminary theoretical analysis. The numerical FEM modeling of FAST/SPS tooling can address this

**ADVANCED** SCIENCE NEWS ADVANCED ENGINEERING MATERIALS

www.advancedsciencenews.com www.aem-journal.com

challenge.<sup>[84,85]</sup> FEM modeling finds nowadays wide application in research and industry to understand, develop, and optimize the FAST/SPS process and tooling.

## 5.1. Basics

Theoretical analysis enables numerical evaluation of thermal, electrical, and mechanical field variables inside a FAST/SPS setup (tooling and sintered part). When the goal of the investigation is temperature distribution at the end of densification, the modeling focuses on the thermal and electrical variables. FAST/ SPS modeling uses the fundamental laws of physics and requires knowledge of the related material properties (Table 6). The material properties must consider the influence of temperature and porosity (for sintered parts). The FAST/SPS model also includes the thermal and electrical resistance of contacts between the tooling elements and the sintered part. Modeling of the electrical field evaluates the current density distribution and the associated heat generation. Modeling of the thermal field provides the temperature distribution inside the FAST/SPS tooling and the sintered part. Modeling of the mechanical field predicts the densification of the sintered part, the punch displacement, and the stress distribution inside the FAST/SPS setup. The simulation of powder densification uses as a rule either the Skorokhod-Olevsky model<sup>[86,87]</sup> or the Abouaf model<sup>[88]</sup> both describing sintering as the viscous flow of porous solids. These models are a modification of the classical von Mises theory of plasticity. [89,90] The Skorokhod-Olevsky and Abouaf models consider the volume change by two independent functions of porosity. The main difference between the Skorokhod-Olevsky and Abouaf approaches is in the determination of porosity functions. The Skorokhod-Olevsky model uses the porosity functions fixed for all types of powder material. In contrast, the Abouaf model assumes the finding of these functions from special experiments. Both models describe the rheological behavior of material with Norton's creep law. [91] This requires the experimental identification of creep parameters.[11,92-94] The more sophisticated models consider grain growth, which affects the densification mechanisms—especially at the end stage of sintering.<sup>[87,88,95]</sup> Several papers describe the basics of FAST/SPS modeling in detail. [96-100] The verification of mechanical stability of FAST/SPS tooling is a less complicated task requiring solution of the regular thermoelastic problem.

## 5.2. Procedure

Typicaly the FAST/SPS modeling uses a FEM software such as ANSYS, ABAOUS, or COMSOL. These packages enable the numerical solution of coupled thermo-electric-mechanical problems. Recently, the Norimat company in France developed a special application for FAST/SPS modeling named Engemini. [101] The modeling includes several steps: 1) the programming of geometry for the FAST/SPS setup or its import from a CAD program; 2) the definition of properties (Table 6) for all tooling elements and the sintered part or their import from a database; 3) the definition contact properties; 4) the meshing of setup parts and contacts; 5) the setting-up of initial conditions, for example, starting temperature; 6) the application of boundary conditions such as heat emission from outer surfaces and heat transfer toward water-cooled electrodes: 7) the application of load (current, voltage, external pressure, punch displacement); 8) the solution of the problem using a virtual PID controller which adjusts the prescribed temperature profile in a reference point<sup>[69,102]</sup>; and 9) the visualization of results. Two types of visualizations are available: the contours showing the distribution of output variables at a certain time point, or the graphs presenting the development of output variables in a specified point over time.

#### 5.3. Accuracy

Accuracy in determining the output parameters is a crucial issue in modeling. Accurate modeling assumes the use of adequate physical and mathematical models, justified assumptions, carefully defined material properties, and proper boundary conditions. Many researchers verified the modeled temperatures in the FAST/SPS tooling meassuring the temperature by thermocouples and pyrometers. [69,103,104] Other authors examined the modeled temperature in the sintered parts by investigating the hardness or microstructure distribution. [13,14,95] The comparison has always shown a reasonable agreement between the modeled and the measured data. Fewer papers examined the modeled current, voltage, and electric power. [69,103–106] Laptev et al., observed a good accuracy for modeling of electrical current and a lower accuracy for voltage modeling. [69]

Table 6. Physical phenomena, related laws, required properties, and output for FAST/SPS modeling.

Field	Phenomenon	Law	Properties	Output
Thermal	Conduction	Fourier's law	Specific heat capacity, thermal conductivity	Temperature
	Radiation	Stefan-Boltzmann law	Emissivity	
	Convection	Newton's law	Heat transfer coefficient	
Electrical	Conduction	Faraday's law	Electrical conductivity	Current, voltage, power
	Heat generation	Joule's law		
Mechanical	Elastic deformation	Young's law	Elastic modulus	Stress, displacement, density
	Viscous flow a)	Norton's law a)	Viscosity <sup>a)</sup>	
	Thermal expansion		TEC b)	

<sup>&</sup>lt;sup>a)</sup>For sintered part; <sup>b)</sup>TEC = thermal expansion coefficient.

on Wiley Online Library for rules of use; OA articles are governed by the applicable Creative Commons

www.aem-journal.com

#### 5.4. Examples

Typical application of FAST/SPS modeling is the optimization of tooling design aiming at a desired temperature distribution within the sintered part. The usual goal is the homogeneous temperature. However, in certain cases, a temperature gradient is required. An example of FAST/SPS is the sintering of functionally graded parts/materials (FGMs). [107–109] The tooling optimization includes several steps. The first step is the temperature simulation with the starting setup geometry. This stage provides initial information about the temperature distribution in the sintered part. **Figure 6** shows an example of such a modeling (Engemini software) for the final dwell at sintering of 316L and SiC discs with a diameter of 50 mm. The SiC disc has a smaller thermal gradient than that of the 316L disc (19 vs. 47 °C). The center of the 316L disc is hotter than the edge, while the center of the SiC disc is colder than the edge.

The second step of modeling considers the application of thermal insulation for the reduction of thermal gradients. The use of thermal insulation is beneficial in this respect, but the insulation increases the cooling time. Wrapping a graphite felt around the die reduces the surface temperature, radiation heat loss, and the radial thermal gradient. The inlay of the CFRC plate between the water-cooled electrodes and the spacer reduces the flow of heat toward the electrodes and the axial thermal gradients. Figure 7 demonstrates the effect of thermal insulation predicted by simulating the temperature field in a 150 mm SiC disc. The use of thermal insulation (graphite felt and CFRC plates) reduces the maximum temperature difference by more than twice during dwell at 1800 °C. However, the temperature gradient is still too high.

The subsequent optimization of tooling geometry (third step of modeling) drastically reduces the temperature inhomogeneity. $^{[81,110]}$  Figure 8 shows that the temperature

difference in the SiC disc declines from 123 to 11 °C after optimization of the height and wall thickness of the graphite die (mold).

# 6. Tooling for Upsizing and Upscaling

Most literature sources describe the application of FAST/SPS in research. However, industry also applied FAST/SPS technology for decades. The transition from research to industrial production usually raises two important aspects: 1) an increase in the size of sintered products (upsizing) and 2) an increase in FAST/SPS productivity (upscaling). Both are closely related to the design of FAST/SPS equipment and the automation of the entire process. Upsizing and upscaling also require the special tooling design.

#### 6.1. Upsizing

The upsizing of FAST/SPS technology often faces a few specific challenges, such as insufficient power of equipment, a long cooling time, inhomogeneous heating of sintered parts, and high tooling costs. Over the last two decades, industry shows a tendency toward manufacturing large FAST/SPS devices. Table 7 presents the series of direct current sintering (DCS) units offered by Thermal Technology LLC (USA). The DCS 500 and DCS 800 furnaces enable the sintering of parts up to 560 mm in size. These are the world's largest FAST/SPS devices. The size of sintered products depends on the requested sintering temperature. [111] In reality, the main factor restricting the size of the sintered parts and the heating rate is the capability of the power source. The application of gas quenching in the sintering chamber reduces the cooling time.<sup>[112]</sup> The more radical way of reducing the cooling duration is to use an external cooling chamber. Proper thermal insulation and a FEM-based

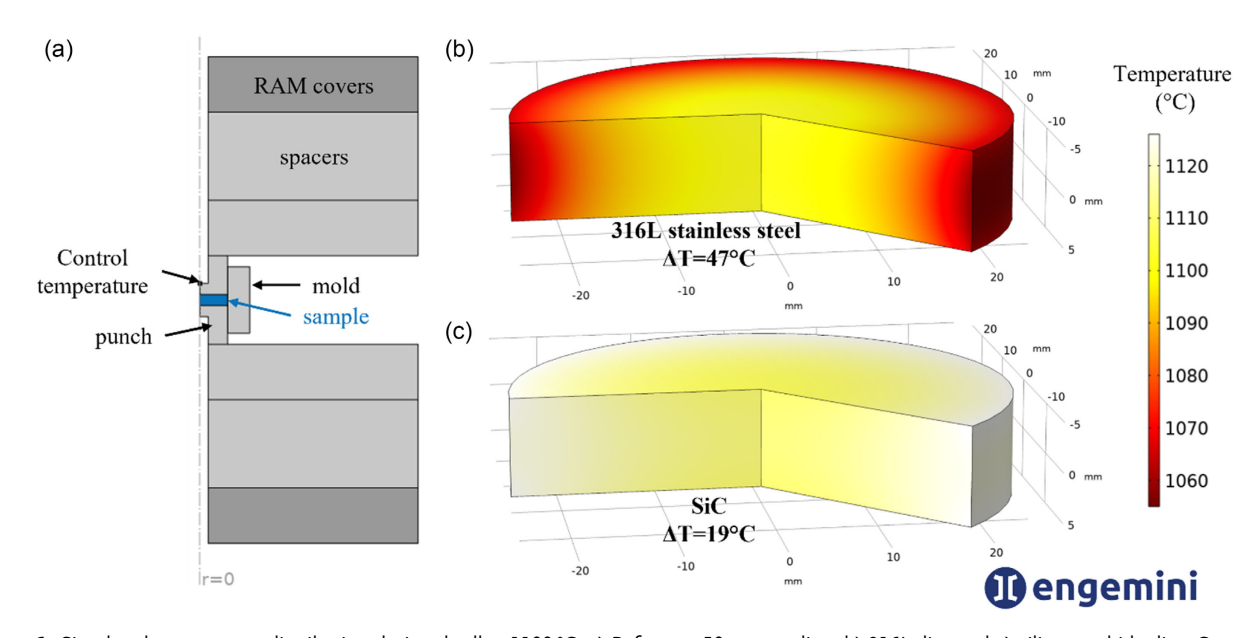


Figure 6. Simulated temperature distribution during dwell at 1100 °C: a) Reference 50 mm tooling. b) 316L disc and c) silicon carbide disc. Courtesy of Norimat SAS.

15272648, 2024, 5, Downloaded from https://onlinelibrary.wiley.com/doi/10.1002/adem/202301391 by Forschungszentrum Jülich GmbH Research Center, Wiley Online Library on [02.05/2024]. See the Terms

onditions) on Wiley Online Library for rules of use; OA articles are governed by the applicable Creative Commons

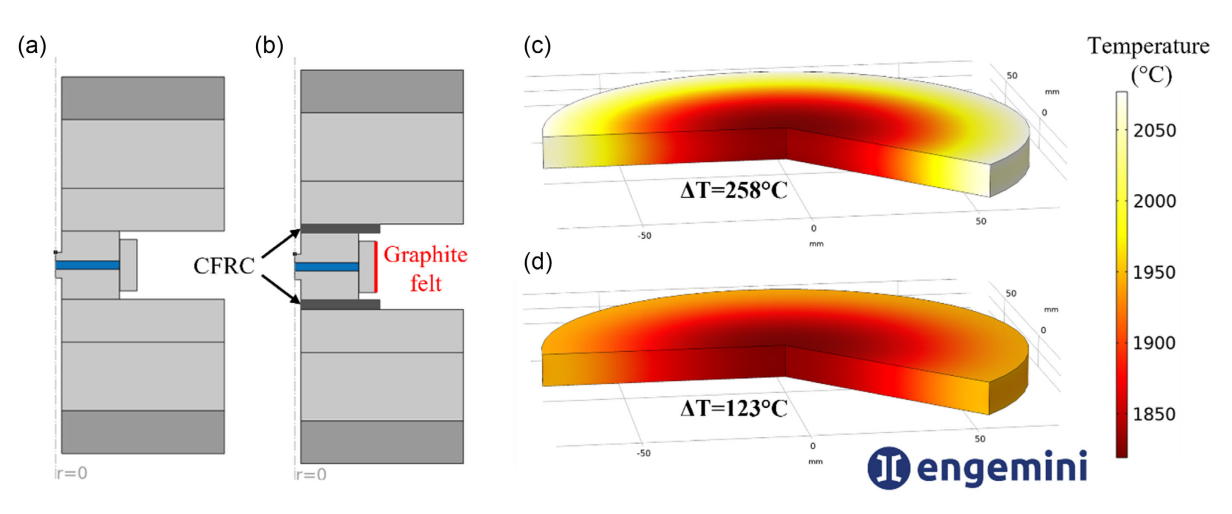


Figure 7. Influence of thermal insulation on temperature distribution in a 150 mm SiC disc during dwell at 1800 °C. a,c) Reference tooling (without insulation). b,d) Tooling with thermal insulation. Courtesy of Norimat SAS.

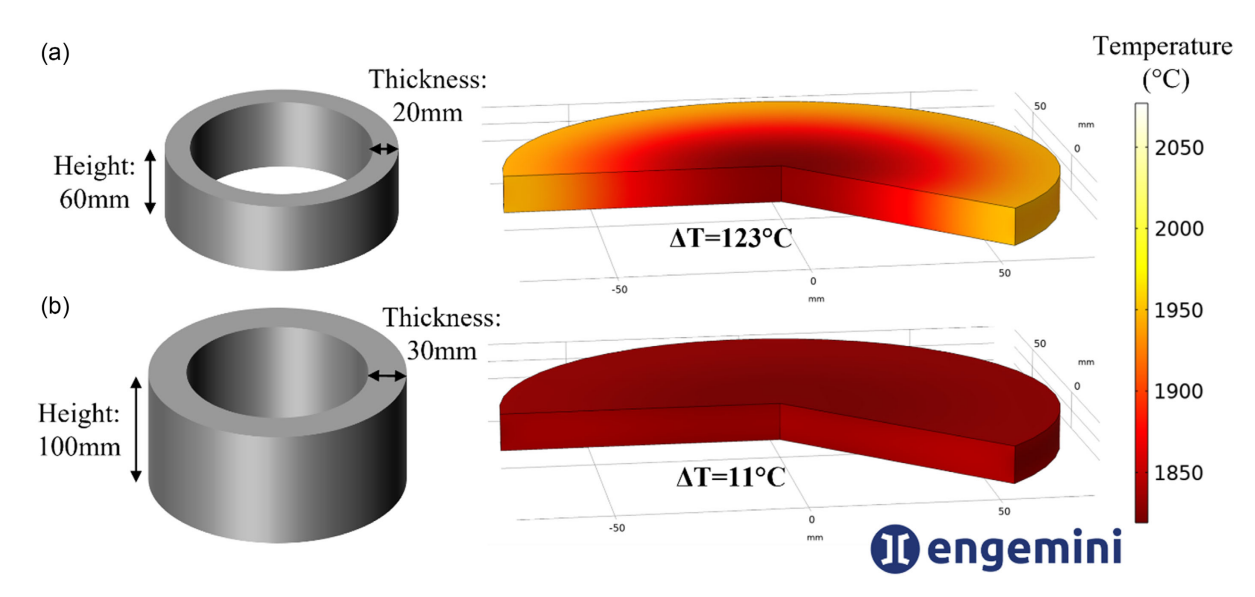


Figure 8. a) Reference and b) geometrically optimized mold with temperature distribution in a SiC sample during a dwell at 1800 °C. Courtesy of Norimat SAS.

Table 7. DCS units offered by Thermal Technology LLC (USA).[111]

Model	Force [kN]	Current [kA]	Typical part size [mm]
DCS 10	100	5	10–50
DCS 25	250	10	10–100
DCS 50	500	20	30–150
DCS 100	1000	30	50–200
DCS 200	2000	50	50–300
DCS 500	5000	150	100–560
DCS 800	8000	150	100–560

optimization of the tooling design might significantly reduce power/energy consumption and improve the temperature uniformity inside the sintered part.<sup>[81]</sup> Another means of reducing the temperature gradients is the application of additional inductive heating as in a hybrid FAST/SPS unit developed by FCT Systeme (Germany). The largest H-HP D 400 hybrid furnace enables the sintering of components with a diameter of up to  $400-450 \ \text{mm}$ . The application of less-expensive graphite grades and changeable inserts reduces the excessive costs of large FAST/SPS tooling.

# 6.2. Upscaling

The literature often considers FAST/SPS as a highly-productive technology. However, this statement is only partly true. Indeed, the heating and holding time at the sintering is only a few minutes, but the FAST/SPS process also includes filling the die, evacuation of the sintering chamber, and cooling. Even in a research-oriented device, the total duration of one FAST/SPS

www.advancedsciencenews.com www.aem-journal.com

cycle is around 1 h. In most cases, the sintering of only one piece per cycle is inefficient for industry. The obvious solution is to sinter as many parts as possible in one run. This is feasible when sintering of cold-pressed powder compacts in a vertically aligned stack (1D), or in multiple dies located in a horizontal plane (2D), or in a tooling combining both these options (3D). **Figure 9**a shows a schematic of a vertical stack with six powder preforms separated by the graphite inserts, and Figure 9b presents a view of such a stack used for sintering brake pads. Mechanical stability and temperature gradient toward the water-cooled electrodes limit the height of the column. Three thermocouples in Figure 9b control the temperature in various parts of the stack. Sintering in a vertical column is especially appropriate for flat powder parts. The use of a die can be avoided if all components in the stack are electrically conductive.

Figure 10a shows a schematic of a setup with multiple dies located in a horizontal plane. This setup is well suited for sintering small and medium powder parts with different configurations. However, after damage of just one die, the entire setup becomes unusable. The application of several small setups with a reduced number of dies addresses this shortcoming. For instance, Dr. Fritsch GmbH uses steel frames to clamp multiple

dies in one set, which also eases the movement of tooling by manipulator in authomated line (Figure 10b).

**Figure 11**a shows a schematic view of an assembly of several dies placed in two layers with a separator in between. In practice, 3D stacks are much larger. Figure 11b shows a stack of brake pads before sintering. In this case, the use of a die is not required, and the graphite plates replace the punches. The extended area of electrodes is beneficial for the mechanical stability of the stack and for the uniform current and temperature distribution. Dr. Fritsch GmbH addresses this issue using large graphite electrodes in their FAST/SPS facilities. For instance, the largest device, MSP 5 (5 MN), has the  $450 \times 450 \times 100 \, \text{mm}^3$  graphite electrodes. [116]

The cooling is usually the longest segment of the FAST/SPS cycle. Therefore, the large-scale production uses the special cooling units located outside the FAST/SPS device. Hereat, the cooling chamber is connected to the FAST/SPS furnace or integrated into a semiautomated line as it is schematically shown in **Figure 12** (Sinter Land Inc. (Japan)). To the best of our knowledge, this is the world's largest semiautomated FAST/SPS line. The line uses a special pallet-type conveyor system for transferring sintered parts between line units. The sintering furnace

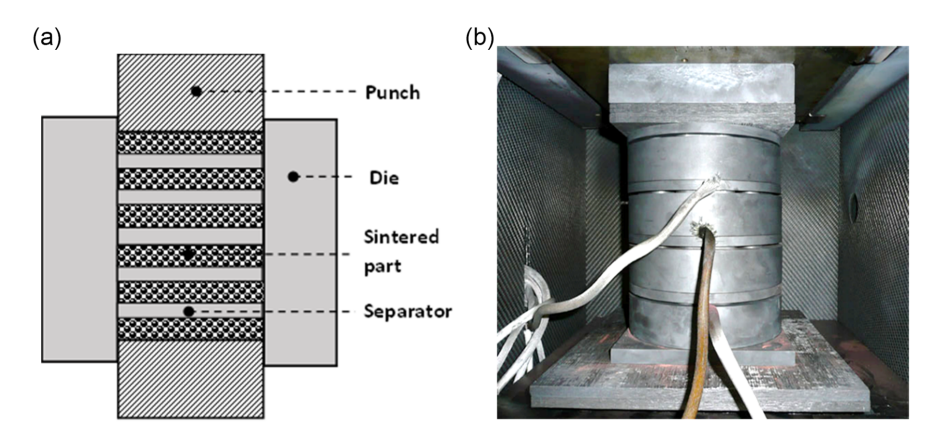


Figure 9. Setup for sintering several preforms in a column. a) Schematic view. b) Setup for sintering brake pads. Courtesy of Dr. Fritsch Sondermaschinen GmbH.

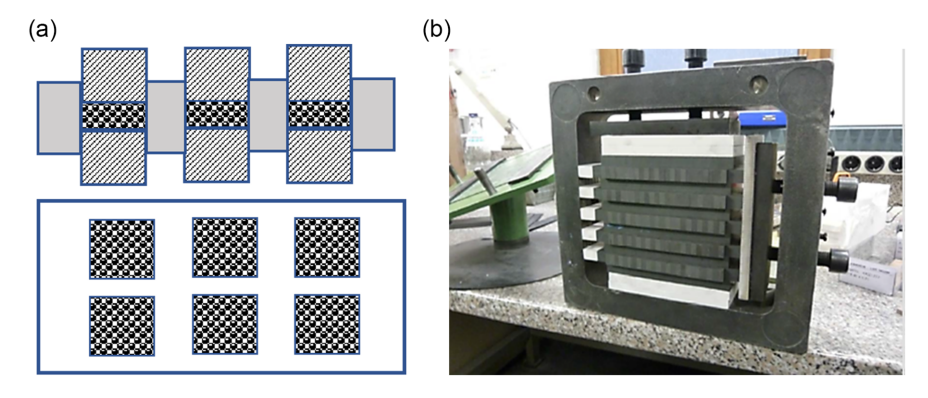


Figure 10. Setup for sintering powder preforms in a multiple die system. a) Cross-section and top view without punches (schematic view). b) Set of multiple dies clamped in a steel frame. Courtesy of Dr. Fritsch Sondermaschinen GmbH.

15272648, 2024, 5, Downloaded from https://onlinelibrary.wiley.com/doi/10.1002/adem.202301391 by Forschungszentrum Jülich GmbH Research Center, Wiley Online Library on [0205/2024]. See the Terms and Conditions

ons) on Wiley Online Library for rules of use; OA articles are governed by the applicable Creative Commons

ENGINEERING



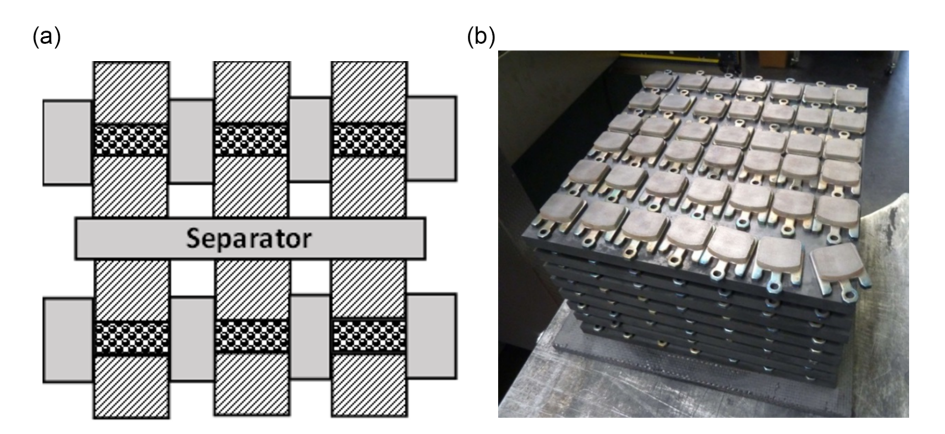


Figure 11. Setup for sintering several preforms in a stack. a) Schematic view. b) Stack of brake pads. Courtesy of Dr. Fritsch Sondermaschinen GmbH.

enables a maximum pressure of 6 MN with a maximum current of 40 kA.[117]

# 7. Tooling for High-Pressure FAST/SPS

The reliable use of FAST/SPS graphite tooling is below 100 MPa. However, the FAST/SPS sintering of certain materials (e.g., transparent ceramics) requires a higher pressure. The use of a graphite grade with an enhanced compressive strength or metallic and ceramic materials can address this issue. This approach is applicable up to a pressure of around 1 GPa. The FAST/SPS community defines sintering with a pressure from 0.1 to 1 GPa as high-pressure FAST/SPS (HP FAST/SPS). Sintering with a pressure of above 1 GPa refers to ultrahighpressure FAST/SPS (UHP FAST/SPS). The UHP FAST/SPS is possible only with a special tooling design.

# 7.1. High-Pressure FAST/SPS

The simplest way of increasing pressure during FAST/SPS is to use a tooling material with a compressive strength higher than that of regular graphite. Practicable options include the use of special grade graphite, tool steels, superalloys, refractory metals, ceramics, or composites. The application area of these materials

depends on sintering temperature, applied load, and other parameters discussed in Section 3.

The literature describes the use of high-strength materials in two types of HP FAST/SPS tooling. The first one is a geometrically regular FAST/SPS tooling (Figure 1) but with all or crucial elements made of a material stronger than graphite. In all cases, the punches must be electrically conductive. The die must be conductive when sintering nonconductive powder and can be nonconductive when sintering electrically conductive powder. Sastry et al., used a standard tooling made of QRO 90 hot work tool steel for the FAST/SPS of Al-Si-Fe-X powders at temperatures up to 500 °C and pressures up to 283 MPa. [118] Gonzalez-Julian et al., performed "cold" FAST/SPS sintering of ZnO nanocrystalline powder at a temperature of 250 °C and a pressure of 300 MPa using a tooling made of W360 tool steel. [83] Ghasali et al., applied an Inconel 718 tooling for the FAST/SPS sintering of Al-VC nanocomposites at a temperature of 220 °C and a pressure of 300 MPa. [119] These data reveal that the FAST/SPS technology does not fully use the potential of steels and superalloys (Section 3). The application of WC-Co tooling enables higher FAST/SPS pressure. Bustillos et al. achieved the full densification of Ti6Al4V powder after lowtemperature sintering at 650 °C in WC-6Co tooling (die and punches) under a pressure of 555 MPa. [120] Shang et al. applied WC-8Co mold for the FAST/SPS sintering of titanium matrix

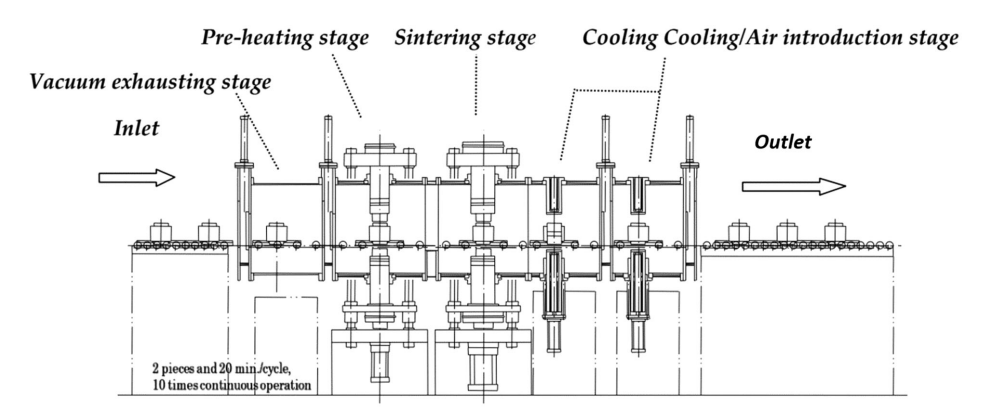


Figure 12. Configuration of a tunnel-type FAST/SPS. Adapted from the paper by Tokita.[117]

nditions) on Wiley Online Library for rules of use; OA articles are governed by the applicable Creative Commons

www.advancedsciencenews.com www.aem-journal.com

composites with a pressure of 300 MPa at a temperature of 850 °C and with a pressure of 200 MPa at a temperature of 950 °C.  $^{[121]}$  Molybdenum and Mo-based alloys such as TZM (Plansee) enable FAST/SPS at higher temperatures. Papynov et al. sintered UO2 pellets in a molybdenum die at 1100 °C and 141 MPa. Using the Mo die instead of a graphite one, the authors minimized UO2 reduction by carbon.  $^{[122]}$  Laptev et al., reported on the sintering of half-cells for solid-state Li-ion battery in TZM tooling at 675 °C and 440 MPa.  $^{[82]}$  Groenwald et al., applied a TZM tool for the FAST/SPS sintering of a Cr2S3 compound at 950 °C and 395 MPa.  $^{[123]}$  A CFRC-based tooling enables higher FAST/SPS temperatures. Xu et al. sintered  $\alpha$ -Al2O3 powder in a CFRC die at a temperature of 925–1550 °C and a pressure varying from 30 to 200 MPa.  $^{[124]}$ 

Anselmi-Tamburini, Munir, and Garay developed and patented a special design of HP FAST/SPS tooling (**Figure 13**). [125,126] The characteristic feature of this tooling is a graphite liner serving as a current conductor and heating element. Another feature is the thick and hard (e.g., binderless WC) insert between internal and external punches. The insert reduces the contact stress on the external graphite punch to an acceptable value. The proposed design enables the use of punches made of nonconductive ceramics. For instance, Anselmi-Tamburini et al., applied a graphite die and nonconductive SiC punches. [126] The authors used HP FAST/SPS for the sintering of fine-grained fully stabilized zirconia (850 °C, 530 MPa), ceria (625 °C, 600 MPa), and samarium-doped ceria (750 °C, 610 MPa). Sokol et al., and Wagner et al., used die, protective discs, and punches made of SiC for FAST/SPS sintering of a magnesium aluminate spinel at a temperature of 1150-1300 °C with a pressure of 150-400 MPa and for sintering of Nd-doped yttrium aluminum garnet (Nd:YAG) ceramics at 1300 °C and 300 MPa. [127,128]

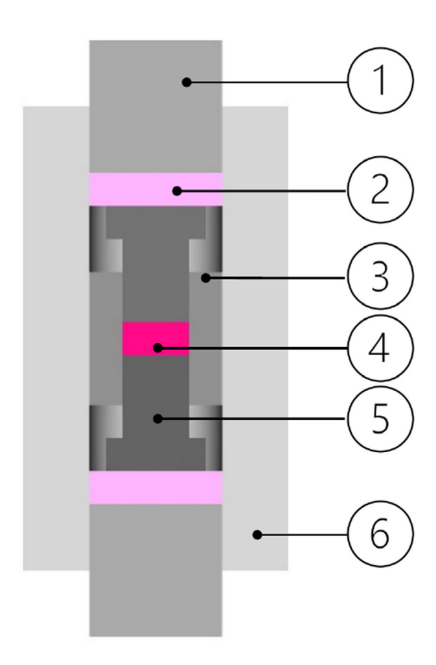


**Figure 13.** Schematic view of an HP-FAST/SPS tooling developed by Anselmi-Tamburini, Munir, and Garay<sup>[125,126]</sup>: 1—graphite electrode, 2—binderless WC spacer, 3—graphite die, 4—sintered part, 5—SiC punch, 6—graphite liner.

Grasso et al., applied a graphite die and electrically conductive binderless WC punches instead of nonconductive SiC punches for the sintering of transparent alumina at a temperature of 900–1150 °C and a pressure of 500 MPa. [129] With these punches, the current path is as in conventional FAST/SPS tooling, and the application of a graphite sleeve becomes redundant. In a further development, Grasso et al., replaced binderless WC with electrically conductive CFRC punches. The authors reported the sintering of transparent alumina at 1000 °C with 400 MPa. [130] The CFRC-based tooling is applicable up to 2000 °C (Section 3).

## 7.2. UHP FAST/SPS

UHP FAST/SPS uses three types of devices adopted from the high-pressure physics and geophysics: multianvil presses, belt-type devices, and Bridgman-type toroidal apparatus. Anvils are the key part of all high-pressure devices, serving as mechanical pressure multipliers. The hardness of the anvil material determines the maximal pressure in a UHP device. The most-used anvil materials are binderless WC (up to 10 GPa) and sintered diamond (above 10 GPa). The UHP FAST/SPS devices use graphite or molybdenum heating elements.

Figure 14 shows a schematic of the concept of a multianvil device. Six anvils synchronically move to the center of a cubic cell, creating quasi-isostatic pressure in a cubic-shaped sample. The multianvil apparatuses use 4, 6, and 8 anvils. The literature refers to the corresponding devices as tetrahedral, cubic, and octahedral presses. The paper by LeGodec and Courac describes the various designs of multianvil presses in detail. [132] Zhou et al., used a UHP cubic cell (with WC anvils) and direct AC heating for the sintering of fine-grained tungsten and molybdenum. A pressure of 9 GPa and a temperature of 1200-1300 °C only enabled full densification of these refractory materials. [133,134] Kuskonmaz et al., sintered γ-Al<sub>2</sub>O<sub>3</sub> without additives in a cubic press at a pressure of 2-7 GPa and temperature varying from 600 to 1200 °C. The authors obtained translucent  $\alpha$ -alumina with a nanosized structure after high-pressure sintering at a temperature of 600 °C and a pressure of 5-7 GPa. [135]

Figure 15a shows a schematic view of the belt-type UHP FAST/SPS device installed at the Institute of Condensed

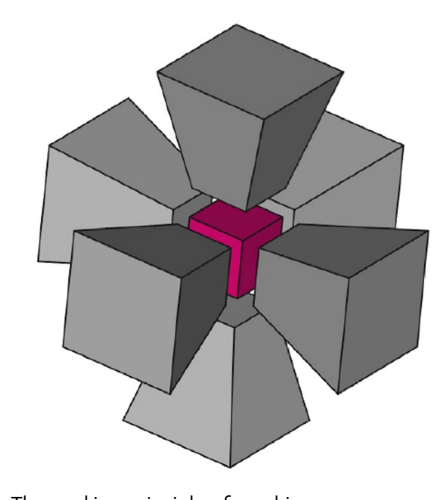


Figure 14. The working principle of a cubic press.

ditions) on Wiley Online Library for rules of use; OA articles are governed by the applicable Creative Commons

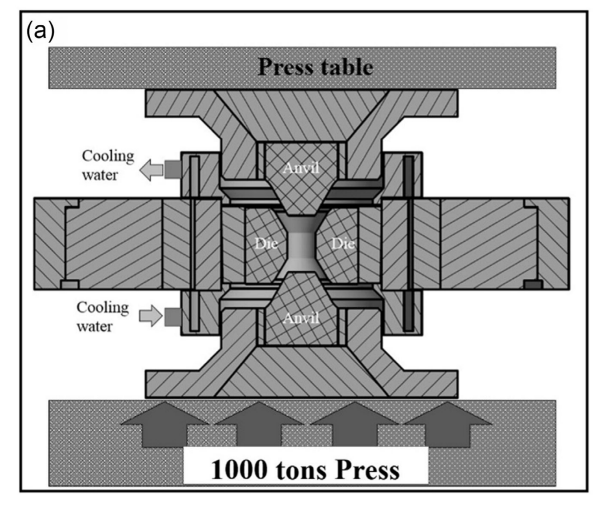
www.advancedsciencenews.com www.aem-journal.com

Matter Chemistry of Bordeaux. [136] This device enables application of a pressure of up to 6 GPa and a temperature of up to 1800 °C for several hours. The apparatus uses a 10 MN press and a pulsed direct current source. The belt-type device includes the tungsten carbide anvils and a tungsten carbide die, prestressed by a steel ring. The second ring contains the channels for water cooling. The wound high-strength steel strip reinforces the entire die/rings assembly. Figure 15b shows a schematic view of the high-pressure cell with a graphite heater. The high-pressure cell uses thermal insulation by the pyrophyllite elements and gaskets. The prepressed pellet in the cell is either in direct contact with the graphite heater or placed within a PTM (graphite, pyrophyllite, sodium chloride, or hexagonal boron nitride). Two molybdenum disks ensure electrical contact while the sandwiching mica ring controls current distribution. Typical sizes of the samples are 10-17 mm in diameter and 3-6 mm in height.[136,137]

**Figure 16** shows the core part of a UHP FAST/SPS toroidal apparatus installed at the Łukasiewicz - Krakow Institute of Technology.  $^{[138]}$  The prepressed powder pellet is inserted into

a deformable cell consisting of a graphite heater and ceramic gaskets. The cell is placed in a hydraulic press equipped with Bridgman-type anvils connecting to a generator of pulsed direct current. The current flows through the graphite heater in the gasket and through the material if conductive. The tungsten carbide toroidal anvils plastically deform the cell, causing a quasi-isostatic pressure inside the sample. With this apparatus, Yung et al., reported the application of a pressure of 7.8 GPa and a temperature of up to 1900 °C. [139] Typical sizes of the samples are 10–15 mm in diameter and 5 mm in height. [138,139]

All UHP FAST/SPS devices utilize indirect temperature control by adjusting the power of the current source. This method requires the power calibration through special experiments. The same is needed for pressure, which is not a linear function of the external load and requires calibration e.g. using the effect of pressure-induced electrical conductivity transition of Ce, Bi, Tl, Yb, or Ba.<sup>[140]</sup> The main application of UHP SPS is the synthesis of expensive products with unique properties such as synthetic diamonds and superhard materials.



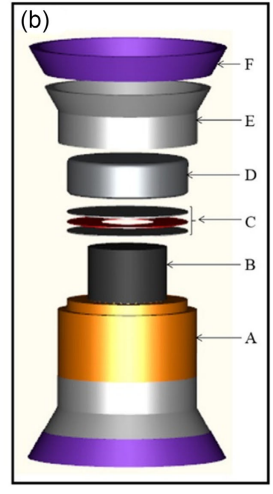


**Figure 15.** a) Belt-type device with two WC anvils and aWC die, four supporting steel rings reinforced by a wound steel strip, and a high-pressure cell inside. b) High-pressure cell: (A) fired pyrophyllite tube, (B) graphite heater with sample inside surrounded by PTM, (C) molybdenum and mica rings, (D) steel cover filled with fired pyrophyllite pellets, (E) raw pyrophyllite gasket, and (F) polymeric gasket. Adopted from the paper by Balima et al.<sup>[136]</sup>

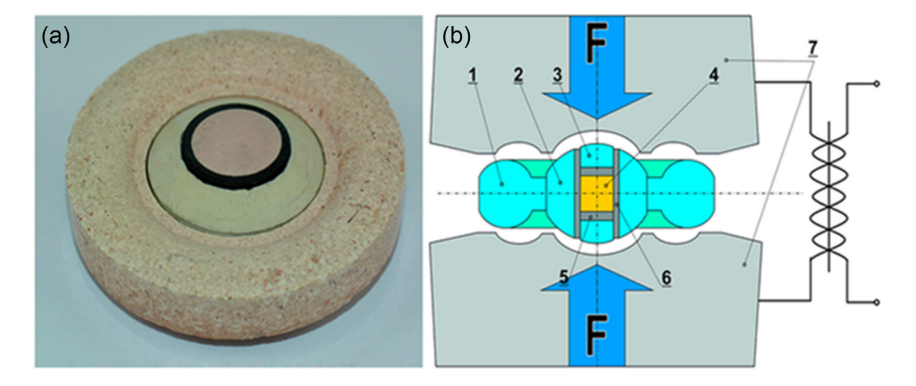


Figure 16. a) Gasket assembly. b) Schematic view of a deformable cell and toroidal anvils: 1,2—ceramic gaskets, 3—ceramic disk, 4—sample, 5—graphite disc, 6—graphite heater, 7—anvils. Adopted from the paper by Knaislová et al.<sup>[139]</sup>

www.advancedsciencenews.com www.aem-journal.com

# 8. Summary and Outlook

Spark plasma sintering, also referred to as Field-assisted Sintering Technique and abbreviated as FAST/SPS, [2] is among a group of pressure-assisted sintering technologies enabling the production of fully dense or nearly dense powder parts. In contrast to HIP or SinterHIP, FAST/SPS uses a graphite, metallic, or ceramic tooling directly heated by electric current due to the Joule effect. Direct resistive heating is the main difference between FAST/SPS and HP applying the external heating elements or inductive heating. In both cases, tooling is the most challenging part of the entire sintering unit. First, the punches and dies in the setup are at the same temperature and mechanical pressure as the sintered part. This issue significantly restricts the choice of tooling materials to that with a high strength at elevated temperatures. In contrast to HP, the FAST/SPS tooling strictly requires the application of electrically conductive materials. The regular tooling material in FAST/SPS is graphite. However, the compressive strength of regular graphite is about 30–50 MPa. Special grades of graphite withstand pressures up to 200–250 MPa, but these grades are expensive. In addition, graphite is an active reductant and carbide former, interacting with many materials at elevated temperatures. Alternatives to graphite are hot work steels, superalloys, molybdenum, and molybdenum alloys. However, the applicability of these materials for FAST/ SPS tooling requires more detailed study. Ceramics or ceramic matrix composites (CMC) are another alternative to graphite. However, most high-temperature ceramics are electrical insulators or semiconductors. Therefore, their application area is the dies for the sintering of electrically conductive materials or inserts in a specially designed tooling. An electrically conductive WC (binderless) ceramic and WC or B<sub>4</sub>C-based conductive composites is an interesting option for FAST/SPS tooling. However, the usability of ceramic materials in FAST/SPS tooling and CMCs requires additional investigation. The drawbacks of ceramic materials are their high price, brittleness, and low resistance to temperature gradients and thermal cycling. A special case is the CFRC composite, which can withstand elevated pressure at extremely high temperatures. However, information about its applicability in FAST/SPS tooling is controversial due to reported brittleness and sensitivity to noncentral loading. This matter requires the additional investigations and experience.

The second challenge with FAST/SPS tooling is its limitations in terms of the shape of the sintered parts to single-level configuration. This limitation originates from the availability of only one moving piston in standard FAST/SPS devices. A possible solution is the tooling with several punches moving separately or the use of sacrificial inserts made of the same material as the sintered part. Another option is the application of QIP in a pressure-transmitting powder media. However, the pressure in a powder bed is inhomogeneous due to the internal friction in the powder medium. This causes the nonuniform densification and shape distortion of sintered part. Therefore, the main application of QIP is sintering of cold-formed, additive-manufactured, or preliminary sintered preforms with high starting density and low shrinkage during FAST/SPS.

The third challenge with the FAST/SPS tooling is the inhomogeneous temperature distribution, especially in the case of

large-sized and/or complex-shaped parts. Proper thermal insulation with the graphite felt and the CFRC inserts in combination with an optimized tooling configuration partly or fully address this challenge. The FEM-assisted tooling design is an effective approach, which is still yet to find its well-deserved place in practice. The optimization of the tooling design also improves energy efficiency. An oversized tooling causes additional power consumption, a limited heating rate, and prolonged cooling. The relationship between the tooling design and the energy demand during FAST/SPS deserves more detailed investigation. [141]

Upsizing (increase in the size of parts) and upscaling (increase in productivity) is the fourth challenge related to FAST/SPS tooling. Both these issues are closely related to advances in the manufacturing of new FAST/SPS equipment. The energetic aspects of the FAST/SPS technology are becoming more crucial to reduce the carbon footprint and fulfill the requirements of the European Green Deal program. Increasing productivity strengthens the need of reproducible quality of the sintered parts. Therefore, an optimization of the tooling design, in the way described in the previous paragraph, is essential for the effective industrialization of FAST/SPS technology.

A special case is the high-pressure (0.1–1 GPa) and ultra-highpressure (over 1 GPa) FAST/SPS tooling. The design of the HP FAST/SPS tooling is identical to that of the regular FAST/SPS tooling. The main difference is that the HP FAST/SPS tooling uses materials with higher strength than conventional graphite. Herein, the application of electrically conductive WC and CFRC punches is promising. However, the practical experience with such punches is still insufficient. The die material in HP FAST/SPS tooling requires special consideration. In many cases, the HP FAST/SPS uses dies manufactured from a high-strength graphite. The high pressure causes the large tensile circumferential stresses in the die wall. At the same time, the tensile strength of graphite is much lower than its compressive strength. The application of graphite dies is therefore risky due to possible fracture at high pressure. This problem requires special investigation, which includes study the tensile strength of graphite. This consideration is also applicable to the ceramic dies due to the low tensile strength of structural ceramics. The UHP FAST/SPS uses the tooling adopted from the high-pressure physics and geophysics. This tooling has a complex design and is suitable for producing of materials with special properties (e.g., synthetic diamonds) and for fundamental research.

# **Acknowledgements**

Open Access funding enabled and organized by Projekt DEAL.

## **Conflict of Interest**

The authors declare no conflict of interest.

# Keywords

field-assisted sintering techniques, modeling, spark plasma sintering, tooling, upscaling

15272648, 2024, 5, Downloaded from https://onlinelibrary.wiley.com/doi/10.1002/adem.202301391 by Forschungszentrum Jülich GmbH Research Center, Wiley Online Library on [0205/2024]. See the Terms and Conditions

and-conditions) on Wiley Online Library for rules of use; OA articles are governed by the applicable Creative Commons



Received: September 1, 2023 Revised: December 14, 2023 Published online: January 21, 2024

- M. Bram, A. M. Laptev, T. P. Mishra, K. Nur, M. Kindelmann, M. Ihrig, J. G. Pereira da Silva, R. Steinert, H.-P. Buchkremer, A. Litnovsky, F. Klein, J. Gonzalez-Julian, O. Guillon, Adv. Eng. Mater. 2020, 22, 2000051.
- [2] O. Guillon, J. Gonzalez-Julian, B. Dargatz, T. Kessel, G. Schierning, J. Räthel, M. Hermann, Adv. Eng. Mater. 2014, 16, 830.
- [3] Z-Y. Hu, Z.-H. Zhang, X.-W. Cheng, F.-C. Wang, Y.-F. Zhang, S.-L. Li, Mater. Des. 2020, 191, 108662.
- [4] M. Tokita, in Handbook of Advanced Ceramics: Materials, Applications, Processing, and Properties (Ed: S. Somiya), Elsevier, Amsterdam, Netherlands 2013.
- [5] T. Robinson, in ASM Handbook (Eds: P. Samal, J. Newkirk), Vol. 7, ASM International, Materials Park, USA 2015.
- [6] A. Litnovsky, F. Klein, X. Tan, J. Ertmer, J. W. Coenen, Ch Linsmeier, J. Gonzalez-Julian, M. Bram, I. Povstugar, T. W. Morgan, Y. M. Gasparyan, A. Suchkov, D. Bachurina, D. Nguyen-Manh, M. Gilbert, D. Sobieraj, J. S. Wróbel, E. Tejado, J. Matejicek, H. Zoz, H. U. Benz, P. Bittner, A. Reuban, Metals 2021, 11, 1255.
- [7] G. Weber, K. Weber, U. Wilkinson, (Dr. Fritsch Sondermaschinen GmbH), DE 10 2020 210 034 B3, 2021.
- [8] Dr. Fritsch Sondermaschinen GmbH, FAST/SPS sintering press LSP-100, https://direktheisspressen.de/fileadmin/user\_upload/ downloads/technical\_specifications/LSP\_100\_e.pdf (accessed: December 2023).
- [9] X. Wei, O. Izhvanov, C. Back, C. D. Haines, D. G. Martin, K. S. Vecchio, E. A. Olevsky, J. Am. Ceram. Soc. 2019, 102, 548.
- [10] C. Manière, E. Torresani, E. A. Olevsky, Materials 2019, 12, 557.
- [11] C. Manière, L. Durand, A. Weibel, C. Estournès, Acta Mater. 2016, 102, 169.
- [12] Y. Kubota, K. Hayakawa, T. Okano, S. Tanaka, T. Nakamura, *Proc. Eng.* 2014, 84, 2421.
- [13] a) A. Couret, J.-P. Monchoux, L. Durand, H. Jabbar, T. Voisin (CNRS), FR 2973265 B1, 2014; b) A. Couret, J.-P. Monchoux, L. Durand, H. Jabbar, T. Voisin (CNRS), US 11045873 B2, 2021.
- [14] T. Voisin, J.-P. Monchoux, L. Durand, N. Karnatak, M. Thomas, A. Couret, Adv. Eng. Mater. 2015, 17, 1408.
- [15] C. Manière, L. Durand, A. Weibel, G. Chevallier, C. Estournès, Scr. Mater. 2016, 124, 126.
- [16] C. Estournès, C. Manière, L. Durand (Université Toulouse III, CNRS), WO 2017/077028 A1, 2017.
- [17] C. Manière, E. Nigito, L. Durand, A. Weibel, Y. Beynet, C. Estournès, Powder Technol. 2017, 320, 340.
- [18] E. A. Olevsky, C. Manière, US 2021/0016499 A1, 2021.
- [19] Z. Shen, H. Peng, M. Nygren, Adv. Mater. 2003, 15, 1006.
- [20] D. Jiang, D. M. Hulbert, J. D. Kuntz, U. Anselmi-Tamburini, A. K. Mukherjee, Mater. Sci. Eng., A 2007, 463, 89.
- [21] F. Wakai, Ceram. Int. 1991, 17, 153.
- [22] K. Vanmeensel, A. Laptev, H. Sheng, I. Tkachenko, O. Van der Biest, J. Vleugels, Acta Mater. 2013, 61, 2376.
- [23] N. S. Weston, M. Jackson, J. Mater. Process. Technol. 2017, 243, 336.
- [24] J. Pope, M. Jackson, Metals 2019, 9, 654.
- [25] N. S. Weston, M. Jackson, Metals 2020, 10, 296.
- [26] R. W. Hailey, US 3356496 A, 1967.
- [27] R. W. Hailey (Wheeling-Pittsburgh Steel Corporation), US 3689259 A, 1972.
- [28] R. Raman, Met. Powder Rep. 1990, 45, 246.
- [29] R. Raman, Met. Powder Rep. 1991, 46, 46.

- [30] S. Hocquet, V. Dupont, F. Cambier, F. Ludewig, N. Vandewalle, J. Eur. Ceram. Soc. 2020, 40, 2586.
- [31] Y. Beynet, R. Epherre (Norimat), EU 3860785 B1, 2022.
- [32] E. A. Olevsky, J. Ma, J. C. LaSalvia, M. A. Meyers, Acta Mater. 2007, 55, 1351.
- [33] E. A. Olevsky, J. Ma, in Advanced in Sintering Science and Technology: Ceramic Transactions (Eds: P. K. Bordia, E. A. Olevsky), Wiley, Hoboken, USA 2010.
- [34] R. Yamanoglu, Powder Metall. Met. Ceram. 2019, 57, 513.
- [35] J. Meng, N. H. Loh, B. Y. Tay, S. B. Tor, G. Fu, K. A. Khor, L. Yu, Scr. Mater. 2011, 64, 237.
- [36] D. V. Dudina, M. A. Legan, N. V. Fedorova, A. N. Novoselov, A. G. Anisimov, M. A. Esikov, *Mater. Sci. Eng.*, A 2017, 695, 309.
- [37] T. P. Mishra, A. M. Laptev, M. Ziegner, S. K. Sistla, A. Kaletsch, C. Broeckmann, O. Guillon, M. Bram, *Materials* 2020, 13, 3184.
- [38] D. V. Dudina, B. B. Bokhonov, Adv. Powder Technol. 2017, 28, 641.
- [39] Entegris Inc., POCO Materials. Graphite properties and characteristics, https://poco.entegris.com/content/dam/poco/resources/reference-materials/brochures/brochure-graphite-properties-and-characteristics-11043.pdf (accessed: December 2023).
- [40] C. Malmstrom, R. Keen, L. Green, J. Appl. Phys. 1951, 22, 593.
- [41] P. Wagner, A. R. Driesner, J. Appl. Phys. 1959, 30, 148.
- [42] C. Manière, G. Lee, J. McKittrick, A. Maximenko, E. A. Olevsky, Carbon 2020, 162, 106.
- [43] SGL Carbon GmbH, SigrafineR7710, https://www.sglcarbon.com/ pdf/SGL-Datasheet-SIGRAFINE-R7710-EN.pdf (accessed: December 2023).
- [44] Entegris Inc., POCO Materials. Typical properties of industrial graphite grades, https://poco.entegris.com/content/dam/poco/shared-product-assets/industrial-grades/specsheet-industrial-table.pdf (accessed: December 2023).
- [45] Mersen, Spark plasma sintering SPS high performance solution, https://www.mersen.com/sites/default/files/publications-media/ 2019-10-spark-plasma-sintering-sps-solutions-mersen.pdf (accessed: December 2023).
- [46] Schunk, Grade FE 879. Data sheet, https://schunk-tokai.pl/en/ wp-content/uploads/e\_FE-879.pdf (accessed: December 2023).
- [47] T. Rodriguez-Suarez, L. A. Díaz, R. Torrecillas, S. Lopez-Esteban, W.-H. Tuan, M. Nygren, J. S. Moya, Compos. Sci. Technol. 2009, 69, 2467.
- [48] M. Moser, S. Lorand, F. Bussiere, F. Demoisson, H. Couque, F. Bernard, Metals 2020, 10, 948.
- [49] G. Bernard-Granger, N. Benameur, C. Guizard, M. Nygren, Scr. Mater. 2009, 60, 164.
- [50] Uddeholms AB, Uddeholm QRO90 supreme, https://www.uddeholm.com/app/uploads/sites/45/2018/01/Uddeholm\_QRO\_90\_supreme\_eng\_p\_1710\_e6.pdf (accessed: December 2023).
- [51] Voestalpine Böhler Edelstahl GmbH & Co KG, Hot work tool steels. Böhler W302 Isobloc, https://www.bohler-edelstahl.com/ app/uploads/sites/92/2023/06/productdb/api/w302-isobloc\_en.pdf (accessed: December 2023).
- [52] Voestalpine Böhler Edelstahl GmbH & Co KG, Hot work tool steels. Böhler W360 Isobloc, https://www.bohler-edelstahl.com/ app/uploads/sites/92/2023/06/productdb/api/w360-isobloc\_en.pdf (accessed: December 2023).
- [53] Plansee S. E. Molybdenum, https://www.plansee.com/download/? DOKNR=HPM-070-TD-026&DOKAR=QM1&DOKTL=100 (accessed: December 2023).
- [54] R. Aalund, in Processing and Properties of Advanced Ceramics and Composites II (Eds: N. P. Bansal, J. P. Singh, J. Lamon, S. R. Choi, M. M. Mahmoud), Wiley, Hoboken, USA 2010.
- [55] L. Silvestroni, L. N. Gilli, A. Migliori, D. Sciti, J. Watts, G. E. Hilmas, W. G. Fahrenholtz, J. Eur. Ceram. Soc. 2020, 40, 2287.

ENGINEERING

www.advancedsciencenews.com www.aem-journal.com

- [56] S. Prochazka, R. J. Charles, in Fracture Mechanics of Ceramics. Vol. 2: Microstructure, Materials and Applications (Eds: R. C. Bradt, D. P. H. Hasselman, F. F. Lange), Springer, New York, USA 1974.
- [57] R. G. Munro, J. Phys. Chem. Ref. Data 1997, 26, 1195.
- [58] L. H. Leipold, in Treatise on Materials Science and Technology. Vol. 9: Ceramic Fabrication Processes (Ed: F. F. Y. Wang), Academic Press, London, UK 1976.
- [59] O. Vasylkiv, D. Demirskyi, D. H. Borodianska, A. Kuncser, P. Badic, Ceram. Int. 2020, 46, 9136.
- [60] D. Garbiec, A. M. Laptev, V. Leshchynsky, M. Wiśniewska, P. Figiel, A. Biedunkiewicz, P. Siwak, J. Räthel, J. Pötschke, M. Herrmann, J. Eur. Ceram. Soc. 2022, 42, 2039.
- [61] F. Klocke, W. König, in Fertigungsverfahren 1. Drehen, Fräsen, Bohren, Springer, Heidelberg 2008.
- [62] K. Vanmeensel, S. G. Huang, A. Laptev, S. A. Salehi, A. K. Swarnakar, O. Van der Biest, J. Vleugels, J. Mater. Sci. 2008, 43, 6435.
- [63] K. Vanmeensel, K. Y. Sastry, A. Laptev, J. Vleugels, O. Van der Biest, Solid State Phenom. 2005, 106, 153.
- [64] L. Melk, M.-L. Antti, M. Anglada, Ceram. Int. 2016, 42, 5792.
- [65] M. Wiśniewska, A. M. Laptev, M. Marczewski, V. Leshchynsky, G. Lota, I. Acznik, L. Celotti, A. Sullivan, M. Szybowic, D. Garbiec, Ceram. Int. 2023, 49, 15442.
- [66] J. Raethel, J. Hennicke, Y. Dyatlova, M. Herrmann, V. Rumyantsev, Adv. Sci. Technol. 2014, 88, 37.
- [67] SGL, Carbon GmbH, https://www.sglcarbon.com/en/marketssolutions/material/sigrabond-carbon-fiber-reinforced-carbon (accessed: December 2023).
- [68] E. Fitzer, L. M. Manocha, in Carbon Reinforcements and Carbon/ Carbon Composites, Springer, Berlin, Germany 1998.
- [69] A. M. Laptev, J. Hennicke, R. Ihl, Metals 2021, 11, 393.
- [70] Carbon Fiber-Reinforced Carbon. Properties, Uses, Forms Supplied, SGL Carbon Group, Meitingen 2004.
- [71] Y. Zheng, J. Zou, W. Liu, W. Wang, W. Ji, Z. Fu, J. Eur. Ceram. Soc. 2023, 43, 5117.
- [72] SGL Carbon GmbH, Sigraflex, https://www.sglcarbon.com/en/markets-solutions/material/sigraflex-flexible-graphite-foil-and-tapes/(accessed: December 2023).
- [73] SGL Carbon GmbH, Sigratherm®, https://www.dhcarbon.co.kr/main\_page/felt.pdf (accessed: December 2023).
- [74] M. Ihrig, R. Ye, A. M. Laptev, Energy Mater. 2021, 4, 10428.
- [75] J. W. Coenen, Y. Mao, S. Sistla, J. Riesch, T. Hoeschen, C. Broeckmann, R. Neu, C. Linsmeier, Nucl. Mater. Energy 2018, 15, 214.
- [76] D. Demirskyi, O. Vasylkiv, Int. J. Refract. Met. Hard. Mater. 2017, 66, 31.
- [77] A. Webb, I. Charit, D. P. Butt, in Spark Plasma Sintering of Materials (Ed: P. Cavaliere), Springer Nature, Cham, Switzerland 2019.
- [78] N. Maity, N. K. Gopinath, K. Biswas, B. Basu, in Spark Plasma Sintering of Materials (Ed: P. Cavaliere), Springer Nature, Cham, Switzerland 2019.
- [79] D. Giuntini, J. Raethel, M. Herrmann, A. Michaelis, E. A. Olevsky, D. Bouvard, J. Am. Ceram. Soc. 2015, 98, 3529.
- [80] M.-R. Ardigo-Besnard, A. Besnard, M. Moser, F. Bussière, Solids 2021, 2, 395.
- [81] A. M. Laptev, M. Bram, K. Vanmeensel, J. Gonzalez-Julian, O. Guillon, J. Mater. Process. Technol. 2018, 262, 326.
- [82] A. M. Laptev, H. Zheng, M. Bram, M. Finsterbusch, O. Guillon, Mater. Lett. 2019, 247, 155.
- [83] J. Gonzalez-Julian, K. Neuhaus, M. Bernemann, J. Pereira da Silva, A. M. Laptev, M. Bram, O. Guillon, Acta Mater. 2018, 144, 116.
- [84] A. Zavaliangos, J. Zhang, M. Krammer, J. R. Groza, *Mater. Sci. Eng., A* 2004, 379, 218.

- [85] K. Vanmeensel, A. Laptev, J. Hennicke, J. Vleugels, O. Van Der Biest, Acta Mater. 2005, 53, 4379.
- [86] E. A. Olevsky, Mater. Sci. Eng., R 1998, 23, 41.
- [87] E. A. Olevsky, C. Garcia-Cardona, W. L. Bradbury, C. D. Haines, D. G. Martin, D. Kapoor, J. Am. Ceram. Soc. 2012, 95, 2414.
- [88] M. Abouaf, J. L. Chenot, G. Raisson, P. Bauduin, Int. J. Numer. Methods Eng. 1988, 25, 191.
- [89] S. Shima, M. Oyane, Int. J. Mech. Sci. 1976, 18, 285.
- [90] A. M. Laptev, Powder Metall. Met. Ceram. 1982, 21, 522.
- [91] E. H. Norton, in Creep of Steel at High Temperatures, McGraw Hill, New York 1929.
- [92] C. Manière, U. Kus, L. Durand, R. Mainguy, J. Huez, D. Delagnes, C. Estournès, Adv. Eng. Mater. 2016, 18, 1720.
- [93] D. Martins, F. Grumbach, C. Manière, P. Sallot, K. Mocellin, M. Bellet, C. Estournès, *Intermetallics* 2017, 86, 147.
- [94] A. Van der Laan, R. Epherre, G. Chevallier, Y. Beynet, A. Weibel, C. Estournès, J. Eur. Ceram. Soc. 2021, 41, 4252.
- [95] S. K. Sistla, T. P. Mishra, Y. Deng, A. Kaletsch, M. Bram, C. Broeckmann, J. Am. Ceram. Soc. 2021, 104, 1978.
- [96] G. Antou, G. Mathieu, G. Trolliard, A. Maître, J. Mater. Res. 2009, 24, 404.
- [97] U. Anselmi-Tamburini, S. Gennari, J. E. Garay, Z. A. Munir, *Mater. Sci. Eng., A* 2005, 394, 139.
- [98] J. Diatta, G. Antou, N. Pradeilles, A. Maître, J. Eur. Ceram. Soc. 2017, 37, 4849.
- [99] C. Manière, L. Durand, G. Chevallier, C. Estournès, J. Mater. Sci. 2018, 53, 7869.
- [100] A. Van der Laan, R. Epherre, C. Estournès, Intermetallics 2022, 141, 107435.
- [101] Norimat, https://www.norimat.com/en/engemini-digital-twin (accessed: December 2023).
- [102] S. Muñoz, U. Anselmi-Tamburini, J. Mater. Sci. 2010, 45,
- [103] A. Pavia, L. Durand, F. Ajustron, V. Bley, G. Chevallier, A. Peigney, C. Estournès, J. Mater. Process. Technol. 2013, 213, 1327.
- [104] K. Vanmeensel, A. Laptev, O. Van der Biest, J. Vleugels, *Acta Mater.* 2007, 55, 1801.
- [105] C. Manière, A. Pavia, L. Durand, G. Chevallier, V. Bley, K. Afanga, A. Peigney, C. Estournès, *Electr. Power Syst. Res.* 2015, 127, 307.
- [106] K. Y. Sastry, K. Vanmeensel, L. Froyen, J. Vleugels, O. Van der Biest, A. Laptev, J. Hennicke, in Euro PM2005 Proc.: Volume 1, EPMA 2005.
- [107] M. Tokita, Mater. Sci. Forum 1999, 308-311, 83.
- [108] S. Decker, L. Krüger, Mater. Des. 2017, 115, 8.
- [109] M. Belmonte, J. Gonzalez-Julian, P. Miranzo, M. I. Osendi, Acta Mater. 2009, 57, 2607.
- [110] T. Vanherck, J. Lobry, G. Jean, M. Gonon, F. Cambier, Int. J. Appl. Ceram. Technol. 2015, 12, E1.
- [111] Thermal Technology, Direct sintering furnace, https://www. thermaltechnology.com/products/dcs-sps-fast (accessed: December 2023).
- [112] F. Zhang, M. Reich, O. Kessler, E. Burkel, *Mater. Today* 2013, 16, 192.
- [113] M. Suárez, A. Fernández, J. L. Menéndez, R. Torrecillas, H. U. Kessel, J. Hennicke, R. Kirchner, T. Kessel, in *Sintering Applications* (Ed: B. Ertuğ), IntechOpen, London, UK 2013.
- [114] FCT Systeme GmbH, https://fct-systeme.de/en/content/4/≈nm. 12≈nc.32/Typ-HP-D-·HHP-D.html (accessed: December 2023).
- [115] J. Hennicke, T. Kessel, S. Rivera Monte, CFI/Ber. DKG 2018, 95, E1.
- [116] Dr. Fritsch Sondermaschinen GmbH, FAST/SPS sintering press MSP 5, https://direktheisspressen.de/fileadmin/user\_upload/ downloads/technische\_spezifikationen/MSP\_5\_e.pdf (accessed: December 2023).

www.advancedsciencenews.com www.aem-journal.com

- [117] M. Tokita, Ceramics 2021, 4, 160.
- [118] K. Y. Sastry, L. Froyen, J. Vleugels, O. Van der Biest, R. Schattevoy, K. Hummert, Mater Sci Forum 2006, 519-521, 1409.
- [119] E. Ghasali, K. Shirvanimoghaddam, M. Alizadeh, T. Ebadzadeh, J. Alloys Compd. 2018, 753, 433.
- [120] J. Bustillos, C. Zhang, A. Loganathan, B. Boesl, A. Agarwal, Adv. Eng. Mater. 2020, 22, 2000076.
- [121] C. Shang, F. Zhang, J. Wang, F. Chen, Compos. A: Appl. Sci. Manuf. 2022, 158, 106981.
- [122] E. K. Papynov, O. O. Shichalin, A. Y. Mironenko, A. V. Ryakov, I. V. Manakov, P. V. Makhrov, I. Y. Buravlev, I. G. Tananaev, V. A. Avramenko, V. I. Sergienko, *Radiochemistry* 2018, 60, 362.
- [123] D. Groeneveld, H. Groß, A.-L. Hansen, T. Dankwort, J. Hansen, J. Wöllenstein, W. Bensch, L. Kienle, J. König, Adv. Eng. Mater. 2019, 21, 1900430.
- [124] H. Xu, J. Zou, W. Wang, H. Wang, W. Ji, Z. Fu, J. Eur. Ceram. Soc. 2021, 41, 635.
- [125] U. Anselmi-Tamburini, Z. A. Munir, J. E. Garay (University of California), US 7601403 B2, 2009.
- [126] U. Anselmi-Tamburini, J. E. Garay, Z. A. Munir, Scr. Mater. 2006, 54, 823
- [127] M. Sokol, S. Kalabukhov, M. P. Dariel, N. Frage, J. Eur. Ceram. Soc. 2014, 34, 4305.
- [128] W. Wagner, B. Ratzker, S. Kalabukhov, S. Kolusheva, M. Sokol, N. Frage, Ceram. Int. 2019, 45, 12279.
- [129] S. Grasso, B.-N. Kim, C. Hu, G. Maizza, Y. Sakka, J. Am. Ceram. Soc. 2010, 93, 2460
- [130] S. Grasso, H. Yoshida, H. Porwal, Y. Sakka, M. Reece, *Ceram. Int.* 2013, 39, 3243.
- [131] Y. Le Godec, S. Le Floch, Materials 2023, 16, 997.
- [132] Y. Le Godec, A. Courac, Materials 2021, 14, 4245.

- [133] Z. Zhou, N. Deng, H. Wang, J. Du, J. Alloys Compd. 2019, 782, 899.
- [134] Z. Zhou, Y. Ma, J. Du, J. Linke, Mater. Sci. Eng., A 2009, 505, 131.
- [135] N. Kuskonmaz, N. Can, A. Can, L. Sigalas, Ceram. Int. 2011, 37, 437.
- [136] F. Balima, F. Bellin, D. Michau, O. Viraphong, A. Poulon-Quintin, U.-C. Chung, A. Dourfaye, A. Largeteau, *Mater. Des.* 2018, 139, 541.
- [137] F. Balima, A. Largeteau, Scr. Mater. 2019, 158, 20.
- [138] D.-L. Yung, S. Cygan, M. Antonov, L. Jaworska, I. Hussainova, Int. J. Refract. Hard. Met. 2016, 61, 201.
- [139] A. Knaislová, P. Novák, S. Cygan, L. Jaworska, M. Cabibbo, Materials 2017, 10, 465.
- [140] M. Prakasam, F. Balima, S. Cygan, P. Klimczyk, L. Jaworska, A. Largeteau, in Spark Plasma Sintering: Current Status, New Developments and Challenges (Eds: C. Estournès, J. Garay, R. Orrù), Elsevier, Amsterdam, Netherlands 2019.
- [141] A. M. Laptev, M. Wiśniewska, M. D. Garbiec, in World PM 2022 Congress Proc., EPMA 2022, p. 188680.
- [142] VDM Metals International GmbH, VDMAlloy 718. Nicrofer 5219 Nb, https://www.vdm-metals.com/fileadmin/user\_upload/Downloads/ Data\_Sheets/Datenblatt\_VDM\_Alloy\_718.pdf (accessed: December 2023).
- [143] H. O. Pearson, in Handbook of Refractory Carbides and Nitrides: Properties, Characteristics, Processing and Application, Noyes Publications, Westwood, NJ 1996.
- [144] S. Sugiyama, S. Sato, H. Taimatsu, J. Jpn. Soc. Powder Powder Metall. 2008, 55, 588.
- [145] M. V. Frandsen, W. S. Williams, J. Am. Ceram. Soc. 1991, 74, 1411.
- [146] K. J. A. Brookes, in World Directory and Handbook of Hardmetals and Hard Materials, International Carbide Data, East Barnet 1996.
- [147] G. A. Gogotsi, Y. L. Groushevsky, O. B. Dashevskaya, Y. G. Gogotsi, V. A. Lavrenko, J. Less-Common Met. 1986, 117, 225.



Alexander M. Laptev received a diploma (1972) and a Ph.D. (1978) from the Bauman Moscow State Technical University. He worked at the Institute for Hydrodynamics in Novosibirsk (Russia) and, after completing the Ph.D. program, at the Donbas State Engineering Academy (Ukraine). He was a visiting scientist and a research associate at Forschungszentrum Jülich (Germany), Katholike Universiteit Leuven (Belgium), Drexel University (USA), and Institut Polytechnique de Grenoble (France). Now, he is with Łukasiewicz – Poznań Institute of Technology (Poland) and an alumnus of Forschungszentrum Jülich. His interests include the theory and practice of sintering with a focus on ceramic matrix composites.



Martin Bram studied materials science at the University Erlangen-Nürnberg (Germany) and received his diploma degree in 1995. He got his Ph.D. in materials science in 1998 from the University of Saarland. Currently, he is working at the Institute of Energy and Climate Research – Materials Synthesis and Processing at Forschungszentrum Jülich (Germany) as a group leader in powder-based processing and sintering. In 2012, he finished his habilitation at Ruhr University Bochum and got a professorship in 2020 there. His main research interests are powder-based processing and sintering of materials for energy applications.



Dariusz Garbiec holds a Ph.D. (2013) and a habilitation (2022) in materials engineering from Poznan University of Technology (Poland). Since the beginning of his scientific career, he has been working on field-assisted sintering technique/spark plasma sintering (FAST/SPS) technology. He initiated and organized several FAST/SPS workshops (2018–2020) in Poland, which evolved in 2021 into an international FAST/SPS conference. In 2022, he was honored with an award from the Minister of Education and Science (Poland) for his scientific achievements and activities. Now, he is the Deputy Director of Research at Łukasiewicz – Poznań Institute of Technology. His research focuses on ceramic materials, particularly carbides and MAX phases.

www.advancedsciencenews.com

www.aem-journal.com



Jan Räthel studied materials science at the Technical University of Ilmenau (Germany). He has been working on the field-assisted sintering technique/spark plasma sintering (FAST/SPS) since 2006. Since 2014, Jan Räthel has been the Heat Treatment Group manager at the Fraunhofer Institute for Ceramic Technologies and Systems. His main fields of interest are technological aspects and upscaling of the FAST/SPS technique, finite-element method-supported tooling design including dimensioning, optimization of sintering processes, and validation.



Matthias Küster studied materials science at the University of Stuttgart (Germany). He worked for several years in the R&D of the automotive industry. Since 2016, he has been with Dr. Fritsch Sondermaschinen GmbH as an application engineer. His responsibilities include design of the FAST/SPS tooling, sintering tests, and customer training.



Olivier Guillon has been the director of the Institute of Energy and Climate Research - Materials Synthesis and Processing at Forschungszentrum Jülich (Germany) since 2014, as well as a full professor at RWTH University Aachen. His interests encompass ceramic processing and sintering, energy technologies such as solid-state batteries, solid oxide fuel/electrolysis cells, gas separation membranes, and others. His achievements have been recognized at the international level (World Academy of Ceramics, fellow of European and American Ceramic Societies). He is the founder and spokesperson of the German expert committee on field-assisted sintering technologies/spark plasma sintering.